

## <sup>230</sup>Th normalization: An essential tool for interpreting sedimentary fluxes during the late Quaternary

Roger Francois,<sup>1</sup> Martin Frank,<sup>2</sup> Michiel M. Rutgers van der Loeff,<sup>3,4</sup> and Michael P. Bacon<sup>1</sup>

Received 11 June 2003; revised 3 November 2003; accepted 20 January 2004; published 5 March 2004.

[1] There is increasing evidence indicating that syndepositional redistribution of sediment on the seafloor by bottom currents is common and can significantly affect sediment mass accumulation rates. Notwithstanding its common incidence, this process (generally referred to as sediment focusing) is often difficult to recognize. If redistribution is near synchronous to deposition, the stratigraphy of the sediment is not disturbed and sediment focusing can easily be overlooked. Ignoring it, however, can lead to serious misinterpretations of sedimentary fluxes, particularly when past changes in export flux from the overlying water are inferred. In many instances, this problem can be resolved, at least for sediments deposited during the late Quaternary, by normalizing to the flux of <sup>230</sup>Th scavenged from seawater, which is nearly constant and equivalent to the known rate of production of <sup>230</sup>Th from the decay of dissolved <sup>234</sup>U. We review the principle, advantages and limitations of this method. Notwithstanding its limitations, it is clear that <sup>230</sup>Th normalization does provide a means of achieving more accurate interpretations of sedimentary fluxes and eliminates the risk of serious misinterpretations of sediment mass accumulation rates. **INDEX TERMS:** 4267 Oceanography: General: Paleoceanography; 4808 Oceanography: Biological and Chemical: Chemical tracers; 4860 Oceanography: Biological and Chemical: Radioactivity and radioisotopes; 4863 Oceanography: Biological and Chemical: Sedimentation; 4866 Oceanography: Biological and Chemical: Sorptive scavenging; **KEYWORDS:** paleoflux, sediment focusing, paleoproductivity

**Citation:** Francois, R., M. Frank, M. M. Rutgers van der Loeff, and M. P. Bacon (2004), <sup>230</sup>Th normalization: An essential tool for interpreting sedimentary fluxes during the late Quaternary, *Paleoceanography*, 19, PA1018, doi:10.1029/2003PA000939.

### 1. Introduction

[2] Reconstruction of oceanic particle fluxes from the sedimentary record is a central part of paleoceanographic research. The information it provides can be interpreted in terms of export production of biogenic material or rates of supply of continental material from aeolian or riverine sources. In this article we review the principle, advantages and limitations of the <sup>230</sup>Th normalization method to interpret the sedimentary record in terms of past changes in the vertical rain rate of particles. We urge the use of this technique as a standard tool in late Quaternary paleoceanographic studies, while identifying its limits and potential errors.

#### 1.1. Problems With the Traditional Approach

[3] Traditionally, fluxes of material to the seafloor have been estimated from mass accumulation rates (MAR) between dated sediment horizons [e.g., *Lyle and Dymond*,

1976; *DeMaster*, 1981; *Curry and Lohmann*, 1986; *Rea and Leinen*, 1988; *Sarnthein et al.*, 1988; *Lyle et al.*, 1988; *Mortlock et al.*, 1991]:

$$\text{MAR} = \rho_{\text{dry}} \times \text{LSR} \quad (1)$$

$$\text{LSR} = (z_2 - z_1) / (t_2 - t_1), \quad (2)$$

where  $\rho_{\text{dry}}$  is the dry bulk density of the sediment ( $\text{g cm}^{-3}$ ), LSR is the linear sedimentation rate ( $\text{cm kyr}^{-1}$ ),  $z_2$  and  $z_1$  are the depths of sediment horizons 2 and 1 (cm), and  $t_2$  and  $t_1$  are the corresponding sediment ages (kyr), generally obtained from <sup>14</sup>C dating or tie points in the  $\delta^{18}\text{O}$  stratigraphy.

[4] Mass accumulation rate of a specific sedimentary constituent (MAR<sub>i</sub>) is then obtained simply by multiplying the total mass accumulation rate by the concentration of the constituent of interest. The latter should be averaged over the entire core section between  $z_1$  and  $z_2$  ( $[i]_{z_1}^{z_2}$ ).

$$\text{MAR}_i = \text{MAR} \times [i]_{z_1}^{z_2} \quad (3)$$

It is important to realize that variations in  $[i]$  between  $z_1$  and  $z_2$  should not be multiplied by the sedimentary rate interpolated between these boundaries to calculate variations in flux, since it cannot be ascertained that the sediment accumulation rate remained constant over the depth interval considered.

<sup>1</sup>Department of Marine Chemistry and Geochemistry, Woods Hole Oceanographic Institution, Woods Hole, Massachusetts, USA.

<sup>2</sup>Department of Earth Sciences, ETH Zürich Institute for Isotope Geology and Mineral Resources, ETH-Zentrum, Zürich, Switzerland.

<sup>3</sup>Alfred-Wegener Institute for Polar and Marine Research, Bremerhaven, Germany.

<sup>4</sup>Now at Rijksinstituut voor Kust en Zee Kortenaerkade 1, The Hague, Netherlands.

[5] Although still widely used, this approach has several major shortcomings: First, the temporal resolution that can be obtained by this procedure is inherently limited by the need to take the difference between two measured ages. Increasing the resolution of the flux record requires dating sediment horizons that are in closer proximity, which automatically increases the relative error on  $(t_2 - t_1)$  and on MAR estimates. Second, MAR calculations rely on knowledge of the dry bulk density of the sediment ( $\rho_{\text{dry}}$ ), which is estimated by sampling and drying known volumes of sediment or by establishing linear or polynomial fits with carbonate concentration [Lyle and Dymond, 1976; Curry and Lohmann, 1986; Froelich et al., 1991]. Either of these approaches is associated with significant uncertainties. Third, and maybe most importantly, MARs thus calculated do not distinguish between the contribution from vertical fluxes originating from the overlying waters, and lateral fluxes resulting from sediment redistribution by bottom currents. Failing to take into account horizontal supply or removal can be very misleading if, as is often the case, MARs are interpreted in terms of fluxes originating from the overlying surface water [e.g., Francois et al., 1993; Pondaven et al., 2000; Marcantonio et al., 2001a; DeMaster, 2002].

## 1.2. The Incidence of Sediment Redistribution on the Seafloor

[6] Sediment redistribution can be either postdepositional or syndepositional. Postdepositional redistribution is due to erosion, transport and redeposition of sediments that have been initially deposited at an earlier time. This is relatively rare and can generally be recognized from disturbed stratigraphy and chronology, clearly ruling out an affected core for reconstruction of fluxes originating from surface water. On the other hand, syndepositional redistribution describes a situation in which resuspension, lateral transport and final deposition occur simultaneous to or soon after initial deposition. Syndepositional redistribution is not always readily identifiable, because the integrity of the sediment stratigraphy and chronology is maintained. As a result, it is often overlooked.

[7] Sediment redistribution on the seafloor occurs on a variety of scales. It can result in large and conspicuous drift deposits (e.g., Feni and Gardar drift in the NE Atlantic; Bermuda Rise in the NW Atlantic; The Meji drift in the NW Pacific), which are often targeted by paleoceanographers because of their high sediment accumulation rates and the high-resolution records they provide. Evidently, the accumulation rates of sediment constituents measured at these sites are not used to reconstruct paleofluxes from the overlying water. However, there is increasing evidence that syndepositional redistribution can occur much more commonly, but more subtly so that it is not so easily recognized.

[8] Recently deposited surficial sediments and particularly phytodetritus that accumulate on the seafloor can be readily redistributed by relatively weak bottom currents [Beaulieu, 2002]. Particle fluxes measured with sediment traps deployed within the bottom boundary layer show evidence for particle “rebound” (i.e., resuspension of particles that have reached the seafloor but have not become incorporated into the sediment; Walsh et al. [1988]). Photographic

evidence shows that phytodetritus accumulates preferentially in small depressions. It can thus be readily surmised that the interaction between bottom currents and small to mesoscale and large topographic features on the seafloor could often and significantly affect accumulation rates without impairing the stratigraphy or chronology of the sedimentary sequences. This is corroborated by high-resolution seismic reflection profiles of the seafloor that often show wide variations in the thickness of layered sediment deposited in the same area. Among many examples, a spectacular illustration of this process was recently reported by Mollenhauer et al. [2002] (Figure 1). The tendency for pelagic and hemipelagic sediments to be winnowed preferentially from topographic highs and deposited preferentially in lows, thus tending to smooth out, over time, underlying roughness in basement topography, has been known since the early days of marine seismic reflection profiling. The process of “syndepositional redistribution” and its effects are well described in the following quotation from Ewing et al. [1964, p. 17] summarizing their observations from crossings of the Mid-Atlantic Ridge: “On the northern and middle crossings, the sediments are mainly in pockets, and intervening areas are almost or entirely bare. A large percentage of the pockets have almost level surfaces. These facts suggest that the sediments deposited on the ridge flow easily after reaching the bottom here. Where impounded, the ridge sediments apparently develop cohesiveness and will not flow easily if subsequently tilted.” An excellent illustration of this sediment “ponding” effect as it occurs on the flanks of the Mid-Atlantic Ridge can be found in the review by Ewing and Ewing [1970, Figure 6]. The distribution of sediments on the Mid-Atlantic Ridge may be an especially dramatic example, but we would submit that it illustrates a process that is widespread, perhaps ubiquitous, in the ocean.

[9] Syndepositional redistribution appears to be particularly common and important in regions with a dynamic bottom water circulation (e.g., Southern Ocean, northern and western Atlantic, equatorial Pacific), where the accumulation rates of laterally redistributed sediments are often many times larger than the fluxes of material sinking from the overlying surface waters [e.g., Suman and Bacon, 1989; Francois et al., 1993; Frank et al., 1999, 2000; Dezileau et al., 2000; Marcantonio et al., 2001a; P. Loubere et al., Lower biogenic fluxes in the eastern equatorial Pacific at the last glacial maximum: Reconstruction of calcite paleofluxes, submitted to *Paleoceanography*, 2003, hereinafter referred to as Loubere et al., submitted manuscript, 2003]. MARs measured by the traditional method in these regions thus often can seriously overestimate the actual settling rates of material from the overlying water column. This problem is compounded by coring biases. The need for high temporal resolution in paleoceanographic reconstructions encourages collection of sediment cores in areas of high accumulation rates, which is achieved with increasing success as surveying and positioning techniques improve. These areas are mostly zones of preferential deposition of redistributed sediment (or sediment focusing). This causes a bias in the available core collections that has resulted in significant overestimates of the sedimentary sink in budget

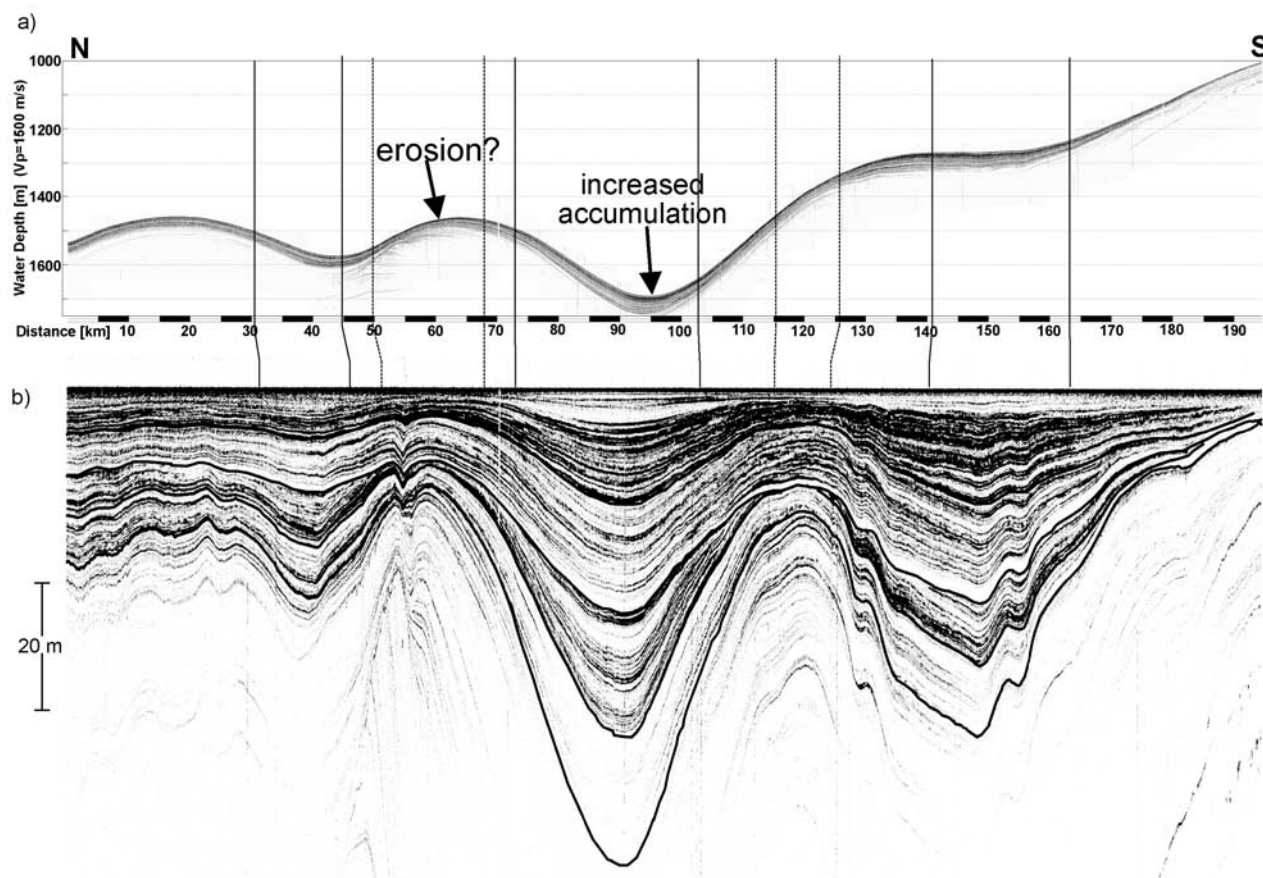


**Figure 1.** Echo sounder profile on a section parallel to the coast of Namibia showing evidence for sediment winnowing and pounding in mesoscale troughs [Mollenhauer *et al.*, 2002].

calculations based on MARs [e.g., Pondaven *et al.*, 2000; DeMaster, 2002], a bias that (again) was well recognized as early as 1964: “New measurements of carbonate deposition are needed in areas of draped sediments, rather than in pockety areas, to establish reliable rates of sediment accumulation” [Ewing *et al.*, 1964, p. 34]. It is thus imperative that a means of identifying and correcting for lateral sediment redistribution be routinely applied, if one is to use correctly the sedimentary record to quantify past variations in particle rain from surface waters.

[10] Bacon and Rosholt [1982], Bacon [1984], Suman and Bacon [1989], and Francois *et al.* [1990] have proposed and developed a method based on normalization to  $^{230}\text{Th}$  to quantify syndepositional redistribution and estimate vertical fluxes from the sedimentary record. A further advantage of this approach is that each  $^{230}\text{Th}$  measurement provides a flux estimate. Thus, unlike the conventional approach of estimating MARs, there is no trade-off between the resolution and precision of the flux estimate, and the resolution at which flux variations can be recognized is limited only by bioturbation. In addition, dry bulk density does not intervene in the flux calculation by  $^{230}\text{Th}$  normalization, thereby eliminating yet another source of error.

[11] Even though the approach was first proposed 20 years ago and its use has been increasing in recent years, its

application is still far from universal, and many recent studies still use MARs to estimate vertical fluxes from late Quaternary sedimentary records [e.g., Ikehara *et al.*, 2000; Thomas *et al.*, 2000; Latimer and Filipelli, 2001; Lyle *et al.*, 2002; Hyun *et al.*, 2002]. Slow acceptance of the  $^{230}\text{Th}$  normalization approach by the paleoceanographic community has been in part the result of contradictory views in the earlier literature regarding the validity of the method’s key underlying assumption. Bacon [1984] argued that the flux of  $^{230}\text{Th}$  scavenged to the seafloor must always be nearly equal to its known production rate in the water column, and thus could be used as a reference to estimate the settling flux of sedimentary particles. However, this view was not universally accepted, particularly during the initial stages of development of the method, and it has been also argued that the flux of  $^{230}\text{Th}$  to the seafloor could considerably exceed production in the water column in regions of high particle flux [Mangini and Diester-Haass, 1983; Scholten *et al.*, 1990; Thomas *et al.*, 2000]. Wider use of the approach may have also been discouraged by the slow sample throughput of the alpha-spectrometric method traditionally used for  $^{230}\text{Th}$  analyses and by the need for somewhat specialized equipment.

[12] These obstacles have now been overcome. Our present understanding of the behavior of  $^{230}\text{Th}$  in the water

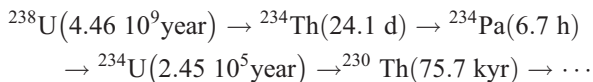
column [Rutgers van der Loeff and Berger, 1993; Scholten et al., 1995, 2001; Moran et al., 1997, 2002; Vogler et al., 1998; Yu et al., 2001; Chase et al., 2003] and recent modeling studies [Henderson et al., 1999; Marchal et al., 2000] provide a stronger basis for asserting the validity while also recognizing the limits of the <sup>230</sup>Th normalization approach. In addition, the development of Inductively Coupled Plasma Mass Spectrometry (ICP-MS) has dramatically improved sample throughput and has replaced alpha-spectrometry for <sup>230</sup>Th measurements in sediments [e.g., Shaw and Francois, 1991; Hinrichs and Schnetger, 1999; Choi et al., 2001; Shen et al., 2002]. The widespread use of this innovative and versatile analytical technique is such that essentially every modern geochemical laboratory now has the wherewithal to measure <sup>230</sup>Th in sediments. The convergence of improved understanding of the geochemical behavior of <sup>230</sup>Th in the ocean and improved analytical capabilities sets the stage for the widespread use of <sup>230</sup>Th normalization in late Quaternary paleoceanographic studies.

## 2. Background: The Marine Geochemistry of <sup>230</sup>Th

[13] The marine geochemistry of <sup>230</sup>Th and its paleoceanographic applications have recently been reviewed [Henderson and Anderson, 2003]. We summarize below aspects that are most relevant to the normalization of sedimentary fluxes.

### 2.1. Continental Weathering

[14] <sup>230</sup>Th (half-life:  $75.69 \pm 0.23$  kyr; Cheng et al. [2000]) is a member of the <sup>238</sup>U decay series. Its parent is <sup>234</sup>U, from which it is produced by  $\alpha$ -decay:



[15] Uranium is present as a minor element in the matrix of most crustal minerals. In old ( $>10^6$  years) undisturbed rocks, the U-decay series within the mineral lattices is in secular equilibrium, i.e., the activity of <sup>230</sup>Th ( $A_{\text{Th-230}}$ ; dpm  $\text{g}^{-1}$ ) is equal to the activity of the preceding isotopes in the decay series ( $A_{\text{Th-230}} = A_{\text{U-234}} = A_{\text{Pa-234}} = A_{\text{Th-234}} = A_{\text{U-238}}$ ). Weathering of crustal rocks disturbs this equilibrium by releasing the more soluble uranium isotopes, while allowing the highly insoluble Th isotopes to be retained. Of the two uranium isotopes, <sup>234</sup>U is released preferentially because of recoil and transmutation from U to Th during <sup>238</sup>U decay, which results in the breaking of chemical bonds and weakening of the mineral lattice [Chabaux et al., 2003]. Weathering thus produces a solution that is comparatively enriched in <sup>234</sup>U ( $A_{\text{U-234}} > A_{\text{U-238}}$ ) but very low in dissolved <sup>230</sup>Th, and a solid residue that is enriched in <sup>230</sup>Th and depleted in <sup>234</sup>U ( $A_{\text{Th-230}} > A_{\text{U-238}} > A_{\text{U-234}}$ ). Subsequent to weathering, if the solid residue is left undisturbed, secular equilibrium is regained at the rate dictated by the half-life of the nuclides. After a period equivalent to about 5 times its half-life ( $\sim 350$  kyr), the <sup>230</sup>Th activity has decayed to near the level of <sup>234</sup>U, while the activity of the latter has gradually increased (with a e-folding time of 248 kyr) to

match that of <sup>238</sup>U. Because of their very short half-lives, <sup>234</sup>Th and <sup>234</sup>Pa regain secular equilibrium with <sup>238</sup>U within a few months or a few days, respectively.

### 2.2. Transport of <sup>230</sup>Th to the Sea

[16] <sup>230</sup>Th is transported from the continents to the sea primarily locked in the mineral lattices of aeolian dust and riverine particles (called hereafter “detrital” <sup>230</sup>Th). On the other hand, uranium is transported to the sea both in dissolved form and locked in lithogenic material as “detrital” uranium.

### 2.3. Production of <sup>230</sup>Th in the Water Column

[17] Dissolved U, added to the sea by rivers and groundwater, resides in the water column for approximately 320–560 kyr before removal in anoxic sediments, biogenic carbonate and at hydrothermal vents [Dunk et al., 2002]. It is thus well mixed in the ocean, displaying conservative behavior such that its concentration in seawater is proportional to salinity. Because of the preferential weathering of <sup>234</sup>U, seawater uranium has a <sup>234</sup>U/<sup>238</sup>U activity ratio of 1.14. For a salinity of 35 permil, seawater <sup>234</sup>U activity ( $^{\text{sw}}A_{\text{U-234}}$ ) is  $2.835 \text{ dpm kg}^{-1}$  [Robinson et al., 2004], corresponding to  $\sim 2910 \text{ dpm m}^{-3}$ . While residing in seawater, <sup>234</sup>U decays and produces <sup>230</sup>Th at a uniform and exactly known rate ( $\beta_{230}$ ) throughout the water column:

$$\beta_{230} = \lambda_{230}^{\text{sw}} \text{ } ^{\text{sw}}A_{\text{U-234}} \\ = 9.16 \cdot 10^{-6} \text{ year}^{-1} \times 2910 \text{ dpm m}^{-3} \\ = 0.0267 \text{ dpm m}^{-3} \text{ year}^{-1}, \quad (4)$$

where  $\lambda_{230}$  is the decay constant of <sup>230</sup>Th.

### 2.4. Removal of <sup>230</sup>Th From the Water Column by Particle Scavenging

[18] Unlike U, Th is highly insoluble in seawater, and <sup>230</sup>Th produced from the decay of dissolved <sup>234</sup>U is promptly removed from the water column by adsorption on settling particles [Bacon and Anderson, 1982]; a process called particle scavenging, which affects all particle-reactive elements. This process can follow two distinct pathways: a vertical pathway (proximal scavenging) due to rapid adsorption on particles settling locally, and a lateral pathway (boundary scavenging) resulting from intensified scavenging at the ocean margins and other regions of high particle flux, after its lateral transport [Spencer et al., 1981]. Partitioning between these two modes of removal is dictated by the residence time (or particle reactivity) of the removed element [Bacon, 1988]. Elements with lesser affinity for particles have longer residence time in the water column and can be transported laterally over longer distances to be preferentially removed by boundary scavenging in high particle flux regions. On the other hand, elements with very high affinity for particles have very short residence times in the water column, which limit the extent to which they can be laterally transported before removal. As a result, they tend to be removed locally by proximal scavenging.

[19] Thorium is among the most particle-reactive elements and is thus rapidly removed from the water column, primarily by proximal scavenging. As a result, the activity

of <sup>230</sup>Th in seawater is nearly four orders of magnitude lower than the activity of its parent <sup>234</sup>U. Typically, its activity increases with depth from <0.1 dpm m<sup>-3</sup> (<2 fg kg<sup>-1</sup>) in the upper water column to ≈1 dpm m<sup>-3</sup> (≈20 fg kg<sup>-1</sup>) at the bottom of the ocean [Nozaki *et al.*, 1981; Bacon and Anderson, 1982]. Its mean residence time in the water column (<sup>sw</sup>τ<sub>scav</sub>), estimated by comparing its activity in seawater (<sup>sw</sup>A<sub>Th-230</sub>) to that of its parent <sup>234</sup>U (<sup>sw</sup>A<sub>U-234</sub>):

$${}^{\text{sw}}\tau_{\text{scav}} = {}^{\text{sw}}A_{\text{Th-230}} / (\lambda_{230} {}^{\text{sw}}A_{\text{U-234}}) \quad (5)$$

ranges from <4 years in the upper water column to ≈40 years in deep water [Anderson *et al.*, 1983]. Since the time required for lateral mixing in a typical ocean basin with a horizontal mixing coefficient of 3·10<sup>7</sup> cm<sup>2</sup> s<sup>-1</sup> [Sarmiento *et al.*, 1982] is ≈100 years, such short residence times indicate that removal of <sup>230</sup>Th by boundary scavenging must be limited, and thus <sup>230</sup>Th removal from the water column must be occurring primarily via the proximal route [Anderson *et al.*, 1990]. If so, the flux of scavenged <sup>230</sup>Th reaching the seafloor with particles settling through the water column (F<sub>230</sub>; dpm m<sup>-2</sup> year<sup>-1</sup>) must always be close to its rate of production over the depth of the overlying water column:

$$F_{230} \approx P_{230} = \beta_{230} \times z, \quad (6)$$

where z is the water depth in meters. This approximation was first proposed by Bacon [1984] and its validity has recently been assessed and largely confirmed in modeling [Henderson *et al.*, 1999; Marchal *et al.*, 2000] and sediment trap [Yu *et al.*, 2001] studies.

## 2.5. <sup>230</sup>Th in Marine Sediments

[20] Sedimentary <sup>230</sup>Th consists of three distinct pools: detrital, scavenged and authigenic.

[21] 1. Detrital <sup>230</sup>Th (<sup>230</sup>Th<sup>det</sup>) is locked in the mineral lattices of erosional debris, and transits rapidly through the water column without interacting with seawater.

[22] 2. Scavenged <sup>230</sup>Th (<sup>230</sup>Th<sup>scav</sup>) is the fraction adsorbed from seawater on the surfaces of sinking particles. Th<sup>scav</sup> is not supported by <sup>234</sup>U in sediment and thus decreases with time (t; kyr) and burial from its initial concentration or activity (<sup>0</sup>A<sub>Th-230</sub><sup>scav</sup>) at the sediment surface with a half-life of 75.7 kyr.

$$A_{\text{Th-230}}^{\text{scav}} = {}^0A_{\text{Th-230}}^{\text{scav}} e^{-(0.693t/75.7)} \quad (7)$$

[23] 3. Authigenic <sup>230</sup>Th (<sup>230</sup>Th<sup>auth</sup>) is produced from the decay of authigenic U that is either adsorbed on oxides or precipitated in anoxic and suboxic sediments after diffusion from bottom waters [Barnes and Cochran, 1990; Klinkhammer and Palmer, 1991]. Most deep-sea sediments deposited under oxic conditions tend not to accumulate authigenic U, but there are documented exceptions where authigenic U is present in deep-sea sediments underlying oxygenated waters [Cochran and Krishnaswami, 1980; Francois *et al.*, 1993; Kumar *et al.*, 1995; Rosenthal *et al.*, 1995; Anderson *et al.*, 1998; Bareille *et al.*, 1998; Frank

*et al.*, 2000; Chase *et al.*, 2001]. Under these circumstances, <sup>230</sup>Th ingrowth starts from the time of authigenic U precipitation according to:

$$A_{\text{Th-230}}^{\text{auth}} = A_{\text{U-234}}^{\text{auth}} \left(1 - e^{-(0.693t/75.2)}\right). \quad (8)$$

## 3. The <sup>230</sup>Th Normalization Method

### 3.1. Principle of the Method

[24] The method of <sup>230</sup>Th normalization proposed by Bacon [1984] relies on the assumption that the flux of scavenged <sup>230</sup>Th reaching the seafloor (F<sub>230</sub>) is known and equal to the rate of <sup>230</sup>Th production from the decay of <sup>234</sup>U in the overlying water column (P<sub>230</sub>). Although only an approximation, this assumption is a priori justified by the very short residence time of <sup>230</sup>Th in the water column and its removal to underlying sediments mainly by proximal scavenging. It is also consistent with the tight inverse relationship between sediment A<sub>Th-230</sub><sup>scav</sup> and accumulation rates first noted by Krishnaswami [1976].

[25] If the flux of <sup>230</sup>Th scavenged from the water column (F<sub>230</sub>) were exactly equal to its rate of production (P<sub>230</sub>), there would be a simple inverse relationship between the settling material's vertical flux (F<sub>V</sub>) and its scavenged <sup>230</sup>Th concentration or activity A<sub>Th-230</sub><sup>scav</sup>:

$$A_{\text{Th-230}}^{\text{scav}} (\text{dpm g}^{-1}) = F_{230} (\text{dpm m}^{-2}\text{year}^{-1}) / F_V \cdot (\text{g m}^{-2}\text{year}^{-1}). \quad (9)$$

Thus, to the extent that F<sub>230</sub> is known (≈β<sub>230</sub> Z), vertical fluxes originating from the overlying water column can be calculated from A<sub>Th-230</sub><sup>scav</sup> measured in sediment. Since Th<sup>scav</sup> decays during burial (equation (7)), a correction must be applied to obtain A<sub>Th-230</sub><sup>scav</sup> at the time of deposition:

$${}^0A_{\text{Th-230}}^{\text{scav}} = A_{\text{Th-230}}^{\text{scav}} e^{(0.693t/75.7)}. \quad (10)$$

This correction requires an independent timescale generally provided by oxygen isotope stratigraphy or <sup>14</sup>C chronology.

[26] Because of its strong adsorption, scavenged <sup>230</sup>Th remains incorporated in the sediment even if the particles that originally transported it to the seafloor are solubilized during early diagenesis. When this occurs, it results in increased <sup>230</sup>Th concentration in the residual sediment. The fluxes calculated by normalizing to the decay-corrected concentration of <sup>230</sup>Th in sediments are thus “preserved” vertical fluxes (<sup>pr</sup>F<sub>V</sub>), i.e., the vertical fluxes of material that remained after diagenetic remineralization:

$${}^{\text{pr}}F_V = \beta_{230} Z / {}^0A_{\text{Th-230}}^{\text{scav}}. \quad (11)$$

The preserved vertical rain rate of any sedimentary constituent i ([<sup>pr</sup>F<sub>V</sub>]<sup>i</sup>) is then:

$$[{}^{\text{pr}}F_V]^i = {}^{\text{pr}}F_V f_i, \quad (12)$$

where  $f_i$  is the weight fraction of constituent  $i$  in the sediment.

### 3.2. Estimating $A_{Th-230}^{scav}$ in Sediment

[27] Applying the <sup>230</sup>Th normalization method thus requires estimation of the activity of scavenged <sup>230</sup>Th ( $A_{Th-230}^{scav}$ ) in the sediment. Analysis of <sup>230</sup>Th in sediment is most often done after total dissolution of the sample, and thus yields total sediment <sup>230</sup>Th ( $A_{Th-230}^{total}$ ), which must be corrected for detrital, and sometimes authigenic, contributions:

$$A_{Th-230}^{scav} = A_{Th-230}^{total} - A_{Th-230}^{det} - A_{Th-230}^{auth}. \quad (13)$$

#### 3.2.1. Estimating $A_{Th-230}^{det}$

[28] It is generally assumed that detrital <sup>230</sup>Th is in secular equilibrium with detrital <sup>238</sup>U:

$$A_{Th-230}^{det} = A_{U-238}^{det}. \quad (14)$$

Sedimentary U measured after total dissolution of the samples ( $A_{U-238}^{total}$ ) consists of two distinct pools: detrital and authigenic. The activity of detrital U ( $A_{U-238}^{det}$ ) is estimated from the activity of <sup>232</sup>Th in sediment ( $A_{Th-232}^{total}$ ), an isotope of Th that is nearly exclusively found in the lithogenic fraction, and the average crustal activity ratio  $A_{U-238}^{crust}/A_{Th-232}^{crust}$  ( $= 0.80 \pm 0.2$ ; *Anderson* [1982]):

$$A_{U-238}^{det} = A_{Th-232}^{total} A_{U-238}^{crust} / A_{Th-232}^{crust}. \quad (15)$$

[29] Alternatively, the  $A_{U-238}^{total}/A_{Th-232}^{total}$  measured in a nearby core devoid of authigenic U could also be used instead of the crustal average [e.g., *McManus et al.*, 1998]. Mean  $A_{U-238}^{det}/A_{Th-232}^{det}$  ratios have also been recently suggested for each ocean basin (Atlantic:  $0.6 \pm 0.1$ ; Pacific:  $0.7 \pm 0.1$ ; Southern Ocean:  $0.4 \pm 0.1$ ; *Henderson and Anderson* [2003]).

#### 3.2.2. Estimating $A_{Th-230}^{auth}$

[30] This requires estimation of the activity of authigenic U by difference.

$$A_{U-238}^{auth} = A_{U-238}^{total} - A_{U-238}^{det} \quad (16)$$

Since authigenic U is derived from seawater,  $A_{U-238}^{auth}/A_{U-238}^{total} = 1.14$ . Thus

$$A_{Th-230}^{auth} = 1.14 A_{U-238}^{auth} \left( 1 - e^{-(0.693t/75.7)} \right), \quad (17)$$

where  $t$  is the time elapsed since emplacement of authigenic U, which is often approximated by the time of deposition of the sediment layer in which it is found.

[31] The general equation to calculate scavenged <sup>230</sup>Th in sediment is thus:

$$A_{Th-230}^{scav} = A_{Th-230}^{total} - \left( A_{U-238}^{det} + 1.14 A_{U-238}^{auth} \left( 1 - e^{-(0.693t/75.7)} \right) \right). \quad (18)$$

[32] Authigenic U is often totally absent in oxic sediment low in Fe and Mn oxides. This is ascertained when

$A_{U-238}^{total}/A_{Th-232}^{total}$  of the sediment sample is similar to that of the average crust. Under these circumstances, equation (18) can be simplified:

$$A_{Th-230}^{scav} = A_{Th-230}^{total} - A_{U-238}^{total}. \quad (19)$$

### 3.3. Estimating Sediment Focusing

[33] If the flux of scavenged <sup>230</sup>Th to the seafloor corresponds to its production rate in the overlying water column and if particles settle through the water column and accumulate on the seafloor without significant syndepositional redistribution, the  $Th_{scav}$  inventory in the sediment between depths  $z_1$  and  $z_2$  should match the production in the overlying column ( $P_{230}$ ) integrated over the time of accumulation of this depth interval, after correction for radioactive decay:

$$\int_{z_2}^{z_1} A_{Th-230}^{scav} \rho dz = \int_{t_1}^{t_2} P_{230} dt. \quad (20)$$

Using this principle, *Suman and Bacon* [1989] defined a focusing factor ( $\Psi$ ) that quantifies syndepositional sediment redistribution:

$$\Psi = \int_{z_2}^{z_1} (A_{Th-230}^{scav} \rho dz) / (P_{230}(t_2 - t_1)) \quad (21)$$

[34] As for MAR calculations,  $\Psi$  can be calculated only as averages between chronological tie points, and variations in  $A_{Th-230}^{scav}$  between tie points should not be translated into changes in the degree of focusing, since the numerator in equation (21) cannot be constrained at this higher resolution. In other words, the degree to which variations in  $\Psi$ , or MAR, can be resolved is limited by the number of sedimentary horizons for which absolute dates can be assigned, a limitation that is sometimes overlooked.

[35]  $\Psi = 1$  indicates that sediments are unaffected by syndepositional redistribution;  $\Psi > 1$  indicates lateral addition of <sup>230</sup>Th and associated sediment, resulting in <sup>230</sup>Th accumulation rates higher than the production rate in the overlying water column (i.e., sediment focusing); and  $\Psi < 1$  indicates lateral removal of <sup>230</sup>Th and associated sediment, resulting in <sup>230</sup>Th accumulation rates lower than the production rate (i.e., sediment winnowing).

[36]  $\Psi \gg 1$  can be found not only in drift deposits [*Suman and Bacon*, 1989; *Thomson et al.*, 1993] but also in areas that are not readily recognized as sites of sediment focusing. This is particularly the case in parts of the Southern Ocean where strong bottom currents prevail [*Petschick et al.*, 1996; *Diekmann et al.*, 1999]. Focusing factors sometimes greater than 10 have been measured in sediment cores from this ocean (e.g., Figure 2; *Francois et al.* [1993]; *Kumar et al.* [1995]; *Frank et al.* [1996, 1999]; *Asmus et al.* [1999]; *Dezileau et al.* [2000]). Significant focusing has also been recognized in the equatorial Pacific

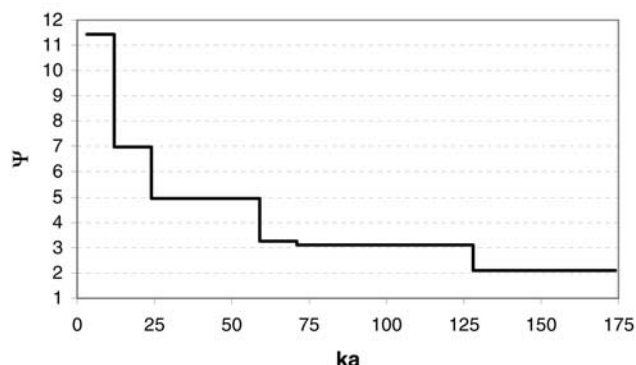


**Figure 2.** Focusing factor ( $\Psi$ ) calculated for a core from the southern Scotia Sea (PS2319;  $59^{\circ}47'S$ ;  $42^{\circ}41'W$ ; 4320 m). The chronology is based on  $^{14}\text{C}$  dates and *C. davisiana* abundance [Diekmann et al., 1999; Gersonde et al., 2003]. Chronology from the latter is established by comparing the *C. davisiana* stratigraphy to a reference core (RC11-120; Hays et al. [1976]). Focusing factors were averaged over core sections corresponding to the main marine isotopic stages (MIS 1–6). Data are available via the PANGAEA database, Alfred-Wegener-Institut für Polar- und Meeresforschung, Columbusstrasse, D-27568 Bremerhaven, Germany (e-mail: info@pangaea.de; Web: <http://www.pangaea.de>).

[Marcantonio et al., 1995, 2001a; Loubere et al., submitted manuscript, 2003] and equatorial Atlantic [Francois et al., 1990; Rühlemann et al., 1996], attesting to the common occurrence of syndepositional sediment redistribution.

[37] When there is no sediment focusing or winnowing ( $\Psi = 1$ ),  $^{230}\text{Th}$  normalized flux ( $^{230}\text{Th}F_V$ , equation (11)) is equal to MAR (equation (1)). If there is syndepositional sediment redistribution,  $^{230}\text{Th}F_V$  diverges from MAR and the latter cannot be used to estimate the former. However, if  $A_{\text{Th-}^{230}\text{Th}}^{\text{scav}}$  in the material transported both vertically and laterally is similar, syndepositional sediment redistribution affects only the  $^{230}\text{Th}$  inventory in the sediment, but not the  $A_{\text{Th-}^{230}\text{Th}}^{\text{scav}}$ . The latter can thus still be used to estimate  $^{230}\text{Th}F_V$  [e.g., Suman and Bacon, 1989; Francois and Bacon, 1991, 1994; Francois et al., 1990, 1993, 1997; Kumar et al., 1993, 1995; Frank et al., 1995, 1996, 1999, 2000; Thomson et al., 1995, 1999; Marcantonio et al., 1996, 2001a; Anderson et al., 1998; McManus et al., 1998; Asmus et al., 1999; J. F. McManus et al., Rapid deglacial changes in Atlantic meridional circulation recorded in sedimentary  $^{231}\text{Pa}/^{230}\text{Th}$ , submitted to *Nature*, 2004, hereinafter referred to as McManus et al., submitted manuscript, 2004]. Overlooking syndepositional redistribution and interpreting MARs indiscriminately as reflecting vertical fluxes from the overlying water can lead to serious errors of interpretation. For instance, glacial maxima in Ba and carbonate MARs in the eastern equatorial Pacific disappear when  $^{230}\text{Th}$  normalization is used [Paytan et al., 1996; Marcantonio et al., 2001a; Loubere et al., submitted manuscript, 2003] (Figure 3). The two records thus lead to very different conclusions regarding climate-related changes in productivity in this important region (Loubere et al., submitted manuscript, 2003). Likewise,  $^{230}\text{Th}$  normalization has recently produced significant revisions in the degree of opal preservation in Antarctic sediments [Pondaven et al., 2000]

and in the importance of the Antarctic Polar Frontal Zone as a sink in the global silica budget [DeMaster, 2002]. Since there are no simple sedimentological means of ruling out, a priori, syndepositional redistribution, normalization to  $^{230}\text{Th}$  should become a prerequisite for evaluating past changes in particle flux from the sedimentary record, if only to verify the absence of such redistribution.

#### 4. Uncertainties and Limits of the Constant $^{230}\text{Th}$ Flux Model

[38] The constant  $^{230}\text{Th}$  flux model is based on several assumptions that we know are not exactly verified. There are also limitations that are inherent to the method. It is thus important to further assess the accuracy of the approach and establish the limits of its applicability.

##### 4.1. Limits Dictated by the Half-Life of $^{230}\text{Th}$

[39] The half-life of  $^{230}\text{Th}$  (75.7 kyr) limits the applicability of the method to sediments that have been deposited in recent years, the potential of using tracers of cosmic dust ( $^3\text{He}$ ) in a similar manner (i.e., assuming that the flux of cosmic dust to the seafloor is constant) has been investigated [Marcantonio et al., 1995, 1996, 2001a, 2001b]. Although a full evaluation of the validity of the approach remains to be done, the initial results comparing  $^3\text{He}$  and  $^{230}\text{Th}$  fluxes in late Quaternary sediments are encouraging and suggest that  $^3\text{He}$  (or other indicators of cosmic dust) could eventually be used to reconstruct  $^{230}\text{Th}F_V$  in sediments too old for the  $^{230}\text{Th}$  method.

##### 4.2. Uncertainties Resulting From the Decay Correction of $^{230}\text{Th}$

[40] Errors in core chronology propagate in the decay-correction and  $^{230}\text{Th}$  normalized flux calculations, but the

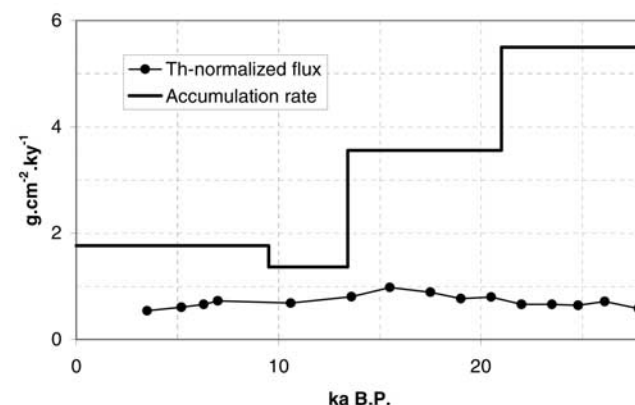


**Figure 3.** Comparison between carbonate mass accumulation rate (MAR) and  $^{230}\text{Th}$  normalized carbonate fluxes obtained from a core in the eastern equatorial Pacific (Y69-71;  $0.1^{\circ}\text{N}$ ;  $86.7^{\circ}\text{W}$ ). Note the lower fluxes and higher resolution obtained by  $^{230}\text{Th}$  normalization. The difference indicates that changes in MAR, particularly the high MARs measured during the LGM, mainly reflect changes in sediment focusing rather than changes in fluxes originating from the overlying surface water (Loubere et al., submitted manuscript, 2003).

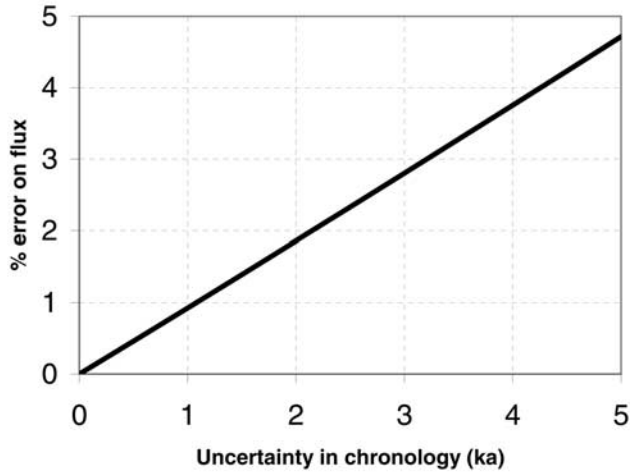


**Figure 4.** Error on <sup>230</sup>Th normalized flux engendered by errors in core chronology.

long half-life of <sup>230</sup>Th results in comparatively small flux errors. For instance, a chronological error of 3 kyr engenders a 2.8% error on the <sup>230</sup>Th normalized flux (Figure 4). On the other hand, similar uncertainties in the chronology delineating a 10 kyr core section would result in 42% uncertainty in the calculated MAR. The relative insensitivity of flux calculations to stratigraphic errors is another advantage of <sup>230</sup>Th normalization over MAR.

**4.3. Uncertainties Inherent to the Algorithm for Flux Calculation**

[41] The algorithm used for flux calculation (equation (8)) is an inverse function, which inherently limits the precision of flux reconstruction when <sup>P</sup>F<sub>V</sub> is high and particularly at shallow depths (Figure 5a). This is not a limiting factor, however, in most deep-sea settings. For instance, with an error of ±0.25 dpm g<sup>-1</sup> in estimating <sup>0</sup>A<sub>Th-230</sub><sup>scav</sup>, the

resulting uncertainty in <sup>P</sup>F<sub>V</sub> in typical deep-sea sediments (Z > 3000 m; <sup>P</sup>F<sub>V</sub>: 10–30 g m<sup>-2</sup> year<sup>-1</sup>) is better than ±10% (Figure 5b).

**4.4. Uncertainties in the Estimation of A<sub>Th-230</sub><sup>scav</sup>**

[42] Equations (14), (18) and (19), used to calculate A<sub>Th-230</sub><sup>scav</sup>, are based on the assumption of secular equilibrium in the lithogenic fraction of marine sediment. We know that this cannot be strictly correct, since weathering causes a disturbance in the isotopic equilibrium between <sup>238</sup>U and <sup>230</sup>Th in crustal material that lasts for more than 10<sup>6</sup> years (see above section on continental weathering). However, in most deep-sea sediments, the activity of scavenged <sup>230</sup>Th is much larger than the activity of detrital <sup>230</sup>Th (A<sub>Th-230</sub><sup>scav</sup> ≫ A<sub>Th-230</sub><sup>det</sup>) and even large errors in estimating A<sub>Th-230</sub><sup>det</sup> increase minimally the error on A<sub>Th-230</sub><sup>scav</sup>. That is not necessarily the case in shallow sediments, where A<sub>Th-230</sub><sup>scav</sup> is lower because of the shallower overlying water column from which <sup>230</sup>Th is scavenged. This problem is compounded in ocean margin sediments, which are often dominated by lithogenic material, resulting in a relatively high A<sub>Th-230</sub><sup>det</sup>. The combined effect of these two factors limits the applicability of the approach in shallow margin sediments.

[43] The presence of authigenic U further limits the precision of A<sub>Th-230</sub><sup>scav</sup> estimates. This is partly because authigenic U concentration can only be calculated approximately from estimates of A<sub>U-238</sub><sup>det</sup>/A<sub>Th-232</sub><sup>det</sup> (equation (15)). In addition, the time of authigenic U emplacement in the sediment cannot be rigorously established from the core chronology. This is because precipitation of authigenic U occurs mainly in the suboxic and anoxic sublayers of the sedimentary column [e.g., Barnes and Cochran, 1990]. Therefore the emplacement of authigenic U occurs somewhat later than the time of deposition of the corresponding sediment horizon [e.g., Francois et al., 1993]. As A<sub>Th-230</sub><sup>scav</sup> decreases with burial (equation (7)) and A<sub>Th-230</sub><sup>auth</sup> increases (equation (17)), the presence of authigenic U limits the applicability of the

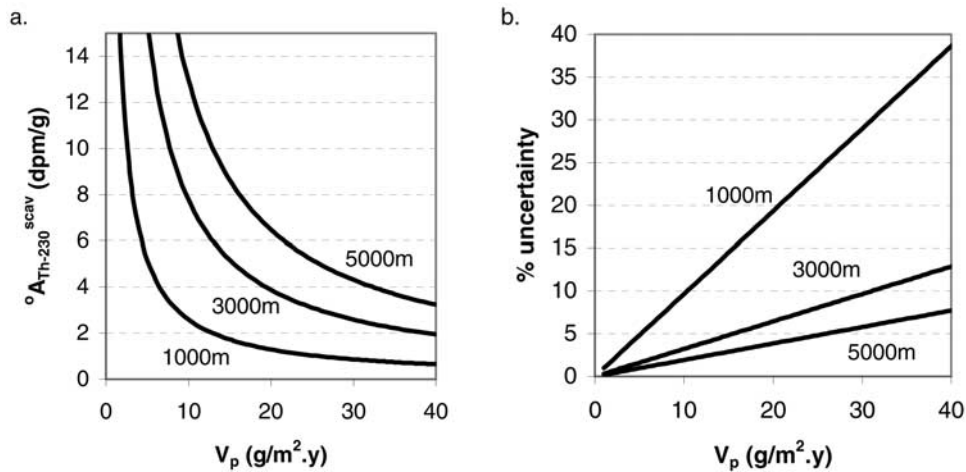


**Figure 5.** (a) Relationship between the scavenged <sup>230</sup>Th activity (<sup>0</sup>A<sub>Th-230</sub><sup>scav</sup>) and vertical settling fluxes of particles (F<sub>V</sub>) at three different depths. <sup>0</sup>A<sub>Th-230</sub><sup>scav</sup> was calculated according to equation (9): <sup>0</sup>A<sub>Th-230</sub><sup>scav</sup> = β<sub>230</sub> Z/F<sub>V</sub>. (b) Uncertainty on estimating vertical settling flux (F<sub>V</sub>) by <sup>230</sup>Th normalization when <sup>0</sup>A<sub>Th-230</sub><sup>scav</sup> has an uncertainty of 0.25 dpm g<sup>-1</sup>.



$^{230}\text{Th}$  normalization approach for older anoxic or suboxic sediments [e.g., Frank *et al.*, 2000]. Development of chemical leaching techniques to directly measure  $A_{\text{Th-230}}^{\text{det}}/A_{\text{U-238}}^{\text{det}}$  and  $A_{\text{U-238}}^{\text{det}}/A_{\text{Th-232}}^{\text{det}}$  in sediment could greatly alleviate these two problems.

#### 4.5. Uncertainties in the Flux of $^{230}\text{Th}$ Reaching the Seafloor

[44] The underlying assumption that the flux of  $^{230}\text{Th}$  scavenged to the seafloor is always exactly equal to the rate of  $^{230}\text{Th}$  production in the overlying water ( $F_{230} = P_{230}$ ) is also an approximation. There are primarily two processes, boundary scavenging and deep water circulation, that can disturb this simple balance.

##### 4.5.1. Boundary Scavenging

[45] If the removal of dissolved  $^{230}\text{Th}$  from the ocean were to occur entirely by proximal scavenging and not by boundary scavenging, as the model assumes, removal would have to be instantaneous, and the activity and residence time of dissolved  $^{230}\text{Th}$  in seawater would have to be zero. Since  $^{230}\text{Th}$  resides in deep water for several decades and its concentration builds up to measurable levels, boundary scavenging must contribute, albeit to a limited extent, to its removal. As a result, the flux of  $^{230}\text{Th}$  should be somewhat higher than the production rate in high particle flux regions, and equation (11) should somewhat underestimate the true preserved vertical rain rate. The opposite should be true for regions of low particle flux.

##### 4.5.2. Deep Water Circulation

[46] Likewise, deviations from constant  $^{230}\text{Th}$  flux could occur as a result of the deep meridional overturning circulation of the ocean (Figure 6). In the absence of significant advection and mixing, a scavenging model that assumes reversible equilibrium between  $^{230}\text{Th}$  adsorbed on particle surfaces and dissolved in seawater predicts linear increase in the  $^{230}\text{Th}$  activity of seawater with depth [Krishnaswami *et al.*, 1976; Nozaki *et al.*, 1981; Bacon and Anderson, 1982] (Figure 6c). However, linear seawater  $^{230}\text{Th}$  profiles are relatively rare, and thus far, they have been found only in subantarctic waters [Rutgers van der Loeff and Berger, 1993; Chase *et al.*, 2003; R. Francois and T. W. Trull, unpublished manuscript, 2003] and in the North Pacific [Roy-Barman *et al.*, 1996; M. P. Bacon and R. Francois, unpublished manuscript, 2003; K. Hayashi, unpublished manuscript, 2002]. Elsewhere, we invariably find significant deviations from linearity, which appear to reflect the influence of deep water formation and upwelling (Figure 6).

[47] In the Nordic Seas, winter cooling of surface water and deep convective mixing result in relatively low and homogeneous  $^{230}\text{Th}$  concentration over the entire water column (Figure 6a) [Moran *et al.*, 1997]. Initiating the meridional overturning (or “conveyor belt”) circulation, this water mass and its low  $^{230}\text{Th}$  concentration forms the Deep Western Boundary Current (DWBC) and the North Atlantic Deep Water (NADW), which propagate southward in the deep Atlantic. The dissolved  $^{230}\text{Th}$  concentration in the newly formed deep water is lower than the concentration in equilibrium with the settling particles predicted by the scavenging model, producing a clear deviation from linearity [Moran *et al.*, 1997, 2002; Vogler *et al.*, 1998] (Figure 6b). The deep water deficit in  $^{230}\text{Th}$  favors desorp-

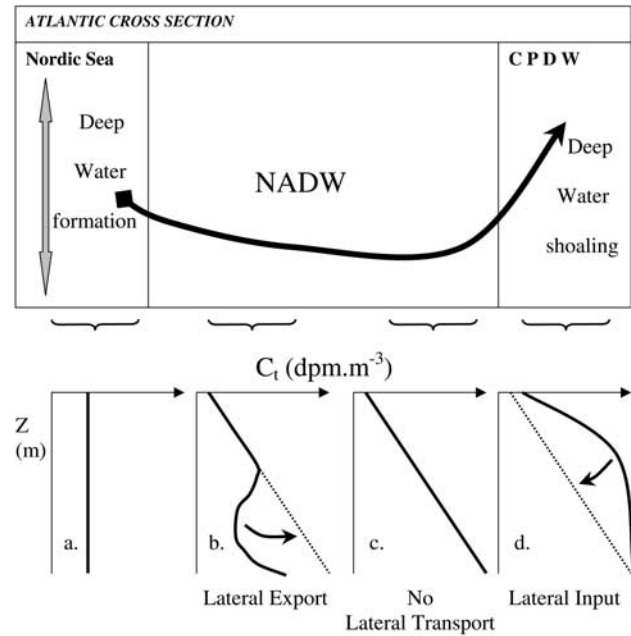


**Figure 6.** Schematic representation of the influence of meridional overturning circulation on  $^{230}\text{Th}$  water column profiles and lateral transport (see text for explanations). The Atlantic cross section shows deep convective mixing in the Nordic Seas and propagation of the North Atlantic Deep Water (NADW) toward the Circumpolar Deep Water (CPDW) in the Southern Ocean. Figures 6a–6d show predicted vertical seawater profiles of total  $^{230}\text{Th}$  ( $C_i$ ) in different oceanic regions (thick continuous line) and the linear profile (dotted line) toward which the profiles are evolving. Arrows indicate the direction of the expected changes in seawater  $^{230}\text{Th}$  activity.

tion of scavenged  $^{230}\text{Th}$  from settling particles, and as deep water flows southward and ages, its  $^{230}\text{Th}$  activity gradually increases with an e-folding time equivalent to the mean residence time of  $^{230}\text{Th}$  with respect to scavenging ( $\approx 20$ –30 years). This gradual increase continues until the linear profile is regained (Figure 6c). Prior to reaching this stage (i.e., in waters with ventilation ages  $< 100$  years), there is net lateral transport of  $^{230}\text{Th}$  “downstream” because at any one site, incoming water always has lower activity than outgoing water. As a result, in areas close to the location of deep water formation, a fraction of  $^{230}\text{Th}$  produced from U decay is used to build-up the  $^{230}\text{Th}$  concentration of the water mass and the vertical fluxes of scavenged  $^{230}\text{Th}$  to the seafloor are lower than the production rate in the overlying water.

[48] In principle the opposite occurs in zones of deep water upwelling and shoaling isopycnals such as found within the Antarctic Circumpolar Current and in the North Pacific. In that situation, we find convex-upward profiles [Nozaki and Nakanishi, 1985; Rutgers van der Loeff and Berger, 1993; Chase *et al.*, 2003; M. P. Bacon and R. Francois, unpublished manuscript, 2003] and  $^{230}\text{Th}$  activity in the water brought up from greater depth is in excess of the value expected from the linear trend dictated by scavenging alone

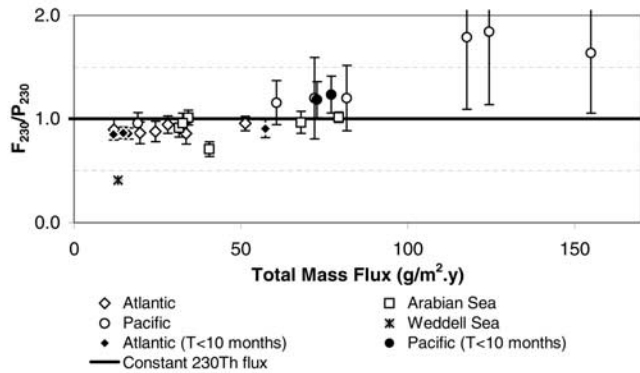


**Figure 7.**  $^{230}\text{Th}$  fluxes intercepted by sediment traps ( $F_{230}$ ) normalized to  $^{230}\text{Th}$  production in the overlying water ( $P_{230}$ ) in oceanic regions characterized by a wide range of total mass flux [Yu *et al.*, 2001].

(Figure 6d). The resulting enhanced adsorption should work toward gradually reducing this excess, thus adding to the scavenged flux of  $^{230}\text{Th}$  and yielding a vertical flux of  $^{230}\text{Th}$  larger than the production rate.

#### 4.5.3. Documenting the Effect of Boundary Scavenging and Deep Water Circulation on the Flux of $^{230}\text{Th}$

[49] Our database on the distribution and fluxes of  $^{230}\text{Th}$  in the water column is rapidly expanding and provides an increasingly accurate and complete view of the extent to which the constant  $^{230}\text{Th}$  flux assumption is valid.

[50] A recent compilation of available sediment trap data [Yu *et al.*, 2001] indicates that the measured flux of scavenged  $^{230}\text{Th}$  normalized to production ( $F_{230}/P_{230}$ ) ranges from 0.8 to 1.7 over most of the ocean (Figure 7). Only in the Weddell Sea, where extensive ice cover limits scavenging [Walter *et al.*, 2001], did  $F_{230}/P_{230}$  drop below 0.7. The highest values were found at the margins of the Pacific Ocean where boundary scavenging is fully expressed. However, these values have high uncertainties ( $1.5 \pm 0.7$ ;  $1.7 \pm 0.8$ ). In parallel, Henderson *et al.* [1999] used a global ocean circulation model that reproduces the major features of ocean circulation and particle flux to evaluate the effect of deep water circulation and boundary scavenging on the scavenged flux of  $^{230}\text{Th}$ . They produced a global map of scavenged  $^{230}\text{Th}$  fluxes ranging from 0.4 to 1.6 times the water column production. In their model, 70% of the ocean floor receives a  $^{230}\text{Th}$  flux within 30% of that expected from production, which is in essential agreement with the sediment trap database.

[51] Using indirect arguments based on correlations between the accumulation rates of different sedimentary constituents, Thomas *et al.* [2000] have argued that the scavenged flux of  $^{230}\text{Th}$  in the equatorial Pacific could far exceed the production rate. They proposed that enhanced  $^{230}\text{Th}$  scavenging in the equatorial upwelling region could result from large but localized, repetitive and transitory increases in particle flux. They argue that such a situation could take place in the equatorial Pacific in response to the passage of tropical instability waves that produces intermittent increases in particle flux [Honjo *et al.*, 1995]. However,

Bacon *et al.* [1985] measured the seasonal variation in  $^{230}\text{Th}$  and total mass flux in the Sargasso Sea over a 3-year period when particle flux variability was as important or larger than observed in the equatorial Pacific and the resulting mean annual flux of scavenged  $^{230}\text{Th}$  was still within 10% of the production rate [Yu *et al.*, 2001]. In addition, Loubere *et al.* (submitted manuscript, 2003) have found large spatial variability in sediment focusing in the eastern equatorial Pacific, which is inconsistent with the interpretation of Thomas *et al.* [2000]. Instead, this spatial variability further points to localized, site-specific sediment redistribution as the main reason for enhanced  $^{230}\text{Th}$  accumulation rates in the sediments of the equatorial Pacific. Compelling geochemical arguments against enhanced  $^{230}\text{Th}$  scavenging in the equatorial Pacific were also presented by Marcantonio *et al.* [2001a]. Although the possible effect of brief, repetitive and localized increase in particle flux on the scavenging of  $^{230}\text{Th}$  and its oceanographic significance should be fully evaluated, it does not appear to significantly affect the general validity of the constant  $^{230}\text{Th}$  flux model.

[52] To illustrate the effect of deep water formation in the North Atlantic, we can make a preliminary calculation using recent water column data that documents the gradual build up in dissolved  $^{230}\text{Th}$  in the Deep Western Boundary Current (Figure 8). The dissolved  $^{230}\text{Th}$  activity in the Denmark Strait Overflow Water (DSOW) off SE Greenland has been measured at  $0.2 \text{ dpm m}^{-3}$  [Moran *et al.*, 1997]. In the core of the DWBC, between 4000 and 5000 m on the lower slope of the N. American margin, dissolved  $^{230}\text{Th}$  activity is  $\sim 0.4 \text{ dpm m}^{-3}$  (R. Francois and M. P. Bacon, unpublished manuscript, 2003). Tritium- $^3\text{He}$  measurements in the DWBC indicate that it takes about 10–12 years for DSOW to travel between the two points [Doney and Jenkins, 1994]. Therefore the core of the DSOW has accumulated  $\sim 0.02 \text{ dpm m}^{-3} \text{ year}^{-1}$ . Considering that the depth range with a noticeable deviation from linearity is about 1000 m, DSOW must have accumulated at most  $20 \text{ dpm m}^{-2} \text{ year}^{-1}$ . Since the rate of production of  $^{230}\text{Th}$  in a 5000 m water column is  $130 \text{ dpm m}^{-2} \text{ year}^{-1}$ , only 15% of the  $^{230}\text{Th}$  produced accumulates in the water mass for export to the south instead of being removed to the underlying sediments. This estimate can be refined as the seawater database in the North Atlantic increases. However, the results already show clearly that little  $^{230}\text{Th}$  can be exported laterally from the North Atlantic as a result of deep water formation.

[53] Figure 6 suggests that we should find a lateral input of  $^{230}\text{Th}$  in the Southern Ocean. In the Atlantic sector, Walter *et al.* [2001] have shown evidence for lateral transport of  $^{230}\text{Th}$  from the Weddell Sea to the Antarctic Polar Frontal Zone (APFZ). The general circulation model study [Henderson *et al.*, 1999] and sediment trap data [Yu *et al.*, 2001] suggest relatively modest lateral addition in the APFZ ( $F_{230}/P_{230} \approx 1.3$ ). However, a more detailed water column study of the distribution and transport of  $^{230}\text{Th}$  in the Pacific sector [Chase *et al.*, 2003] indicates that lateral addition from upwelling in the Antarctic Circumpolar Current maybe compensated by a northward export resulting from deep water formation near the Antarctic continent, resulting in scavenged  $^{230}\text{Th}$  fluxes similar to production rates, at least in the western Pacific sector.

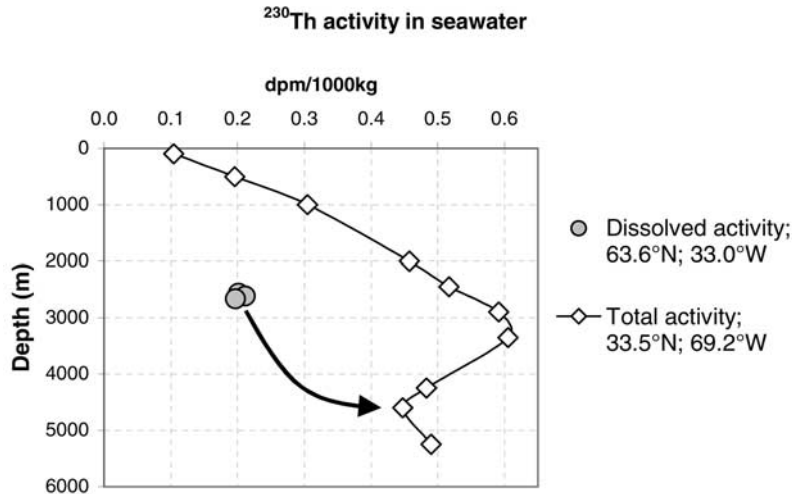


**Figure 8.** Increase in  $^{230}\text{Th}$  activity in the Deep Western Boundary Current between Denmark Strait (63.6°N; 33.0°W; dissolved  $^{230}\text{Th}$  activity; Moran *et al.* [1997]) and a station off New England (33.5°N; 69.2°W; total  $^{230}\text{Th}$  activity; R. Francois and M. P. Bacon, unpublished manuscript, 2003).

[54] Assumption of constant  $^{230}\text{Th}$  flux in regions where  $F_{230}/P_{230} > 1$  will underestimate the preserved vertical rain rate and thus overestimate sediment focusing. The errors will be systematically in the other direction for  $F_{230}/P_{230} < 1$ . Water column profiles, sediment trap fluxes and modeling studies suggest, however, that  $F_{230}/P_{230}$  rarely drops below 0.7, i.e., that the constant flux model will engender systematic errors generally not exceeding 30%, although in some restricted regions, such as the Weddell Sea, they could be larger. Likewise,  $F_{230}/P_{230}$  seems rarely to exceed 1.5 [Henderson *et al.*, 1999; Yu *et al.*, 2001], suggesting maximum errors of  $\approx 50\%$  in high flux regions. These errors are small compared to potential corrections required for syndepositional redistribution of sediments (up to  $>1000\%$ ; Figure 2). The constant flux model proposed by Bacon [1984] is thus a robust and useful approximation. Downcore records of flux variability reconstructed by  $^{230}\text{Th}$  normalization will be somewhat muted, since higher fluxes tend to be underestimated and lower fluxes overestimated, but Figure 7 indicates that this effect will be small compared to the recorded flux variations (a ten-fold increase in particle flux is required to double the flux of scavenged  $^{230}\text{Th}$ ). Because these biases are systematic and not random, as we gain a more quantitative understanding of the factors that control the lateral transport of  $^{230}\text{Th}$  in the water column, it will eventually be possible to take these deviations into account, thereby further increasing the accuracy of the  $^{230}\text{Th}$  normalization method.

#### 4.6. Uncertainties in the Correction For Syndepositional Sediment Redistribution

[55] Even with a perfect constant flux tracer, uncertainties would remain when applied to the reconstruction of vertical flux from sediments affected by sediment redistribution. These uncertainties result in part from possible differences in the composition of the sediment laterally and vertically transported, and in part from ambiguities in the meaning of “vertical flux.”

#### 4.6.1. Modes of Syndepositional Redistribution of Sediment

[56] Syndepositional sediment redistribution can follow two distinct pathways (Figure 9):

[57] 1. Intermediate nepheloid transport, where sediment resuspension is initiated at shallower depth ( $Z_i$ ) from topographic highs (continental slopes, Mid Ocean Ridges, seamounts) and is followed by lateral transport of the fine resuspended particles along isopycnals over relatively long distances ( $\Delta H$ ) prior to capture by large particles from surface water and incorporation into the vertical settling flux.

[58] 2. Bottom nepheloid transport, resulting from resuspension of bottom sediments within the zone of turbulent mixing above the seafloor. Here, the water depth at which resuspension occurs ( $Z_i$ ) is close to the depth of final deposition ( $Z_f$ ), and lateral transport can occur over a wide range of distances ( $\Delta H$ ).

[59] There is a continuum of depth differential ( $\Delta Z = Z_f - Z_i$ ) between zones of initial resuspension ( $Z_i$ ) and final deposition ( $Z_f$ ). The vertical flux originating from the surface mixed layer ( $F_V$ ) is distinct from the lateral flux of particles ( $F_L$ ) that is being added to the vertical flux at depth  $Z_i$ . The total flux ( $F_T$ ) is the sum of the initial vertical flux from the surface mixed layer plus the cumulative horizontal flux ( $\Sigma F_L$ ):

$$F_T = F_V + \Sigma F_L. \quad (22)$$

[60] The flux originating from the mixed layer ( $F_V$ ) is often the flux of interest to paleoceanographers because of its direct link with export production from the euphotic zone, and is the quantity that often we want to estimate by  $^{230}\text{Th}$  normalization.

#### 4.6.2. The Effect of Sediment Redistribution on $^{230}\text{Th}$ Normalized Fluxes

[61] If particles settling directly from the overlying water and particles that have been laterally redistributed

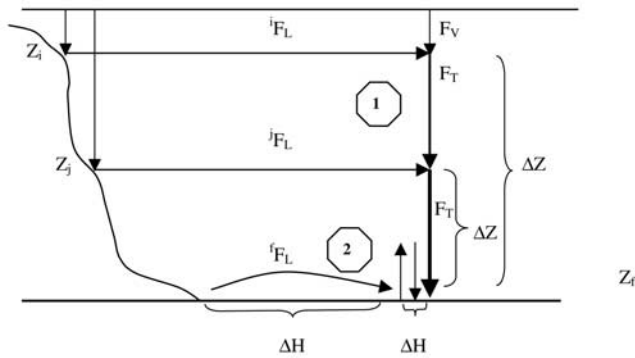


**Figure 9.** Modes of syndepositional sediment redistribution: (1) Intermediate nepheloid transport. (2) Bottom nepheloid transport.  $Z_{i,j,\dots}$  are the depth of initial resuspension of the laterally transported sediment.  $Z_f$  is the depth of final deposition.  $\Delta H$  and  $\Delta Z$  are the lateral and vertical distances separating the sites of initial resuspension and final deposition.  $F_V$  is the vertical flux originating from surface mixed layer.  ${}^i F_L$  is the contribution to the vertical flux that is laterally transported at depth  $Z_{i,j,\dots}$ .  $F_T$  is the total flux ( $F_T = F_V + \Sigma F_L$ ). Only a fraction of  $F_T$ ,  $F_V$  and  $F_L$  are preserved and buried in sediment. The resulting preserved fluxes are denoted  ${}^{Pr}F_T$ ,  ${}^{Pr}F_V$  and  ${}^{Pr}F_L$ .

have similar  $^{230}\text{Th}$  activities, the constant  $^{230}\text{Th}$  flux model (equation (11)) can readily yield the preserved flux originating from surface waters ( ${}^{Pr}F_V$ ) and accurately estimate  $\Psi (= {}^{Pr}F_T / {}^{Pr}F_V)$ , where  ${}^{Pr}F_T$  is the total preserved flux, i.e., the sum of the vertical and integrated lateral fluxes preserved during burial). These conditions are met when the sediment is redistributed by bottom nepheloid transport on a relatively flat seafloor within a region of uniform settling flux. This situation arises when interaction between bottom currents and small to mesoscale irregularities on the seafloor creates localized zones of reduced current velocity where particles preferentially settle (Figure 1). Then the  $^{230}\text{Th}$  activity of the sediment that initially settled within the zone of redistribution is the same everywhere, and sediment redistribution will not change the  $^{230}\text{Th}$  concentration in focused sediments. This type of local to mesoscale sediment redistribution is likely to be prevalent wherever bottom currents are sufficiently high to redistribute particles that just settled on the seafloor ( $\sim 10 \text{ cm s}^{-1}$ ; *Beaulieu* [2002]).

[62] In contrast, redistribution of sediment through intermediate nepheloid layers (Figure 9) can produce inaccuracies in  $^{230}\text{Th}$ -based estimates of  ${}^{Pr}F_V$ . The fine particles initially resuspended at shallower depth ( $Z_i$ ) should be in equilibrium with seawater as they are carried along isopycnals, thereby laterally transporting scavenged  $^{230}\text{Th}$ . Once these particles are incorporated into the vertical settling flux, they start contributing to the scavenging of dissolved  $^{230}\text{Th}$  from seawater at depth  $> Z_i$ . This lowers the dissolved  $^{230}\text{Th}$  activity in deeper water and the  $^{230}\text{Th}$  activity of settling particles below the values that would have been attained without lateral transport. As a result, the fluxes obtained by  $^{230}\text{Th}$  normalization are intermediate between preserved fluxes originating from the surface ( ${}^{Pr}F_V$ )

and the total preserved flux ( ${}^{Pr}F_T$ ). If resuspension and lateral transport occur close to the seafloor (i.e., as  $Z_i$  approaches  $Z_f$ ),  $^{230}\text{Th}$  normalized fluxes provide accurate estimates of the preserved vertical flux originating from the surface mixed layer. On the other hand, if lateral transport originates from shallow depths (e.g., horizontal transport within intermediate nepheloid layers originating from the shelf break; *Pak et al.* [1980]; *Dickson and McCave* [1986]),  $^{230}\text{Th}$  normalized fluxes are a more accurate estimate of the total preserved fluxes ( ${}^{Pr}F_T = {}^{Pr}F_V + \Sigma {}^{Pr}F_L$ ).

[63] The error on  ${}^{Pr}F_V$  due to lateral transport within deep nepheloid layers is thus typically small in comparison to the extent of sediment focusing often observed [*Francois et al.*, 1990]. For instance, if we assume uniform lateral transport within the bottom 1000 m of a 5000 m water column that triples sediment accumulation rates to  $30 \text{ g m}^{-2} \text{ year}^{-1}$  from a  ${}^{Pr}F_V$  of  $10 \text{ g m}^{-2} \text{ year}^{-1}$ ,  $^{230}\text{Th}$  normalized fluxes overestimate  ${}^{Pr}F_V$  by only 23% compared to 200% for MARs, and the focusing factor ( $\psi$ ) is underestimated by 19%. However, if the resuspended sediment originates from an oceanic province where the composition of settling particles is distinct from that at the site of final deposition, deep nepheloid transport can produce larger errors in the  ${}^{Pr}F_V$  of individual sediment constituents. This could occur when nepheloid layers consist of lithogenic particles that have been resuspended from the continental slope [*Biscaye and Eittrheim*, 1977; *McCave*, 1986]. Such lateral addition increases the  $^{230}\text{Th}$  normalized lithogenic fluxes above the vertical flux originating from the overlying surface waters, while decreasing slightly the  $^{230}\text{Th}$  normalized fluxes of biogenic material below the actual rain rate. On Bermuda Rise, for instance, where a well-studied drift deposit is accumulating, two different cores were analyzed, one by *Suman and Bacon* [1989] [KNR 31 GPC5] and the other by *McManus et al.* (submitted manuscript, 2004) [OC326 GGC 5]. Although taken in close proximity, the two cores have different mean Holocene sedimentation rates (GPC 5:  $19 \text{ cm kyr}^{-1}$ ; GGC 5:  $9 \text{ cm kyr}^{-1}$ ), further illustrating the large variations in sediment accumulation rate that can exist within short distances on the seafloor. Notwithstanding the large difference in sedimentation rate, both cores give the same  $^{230}\text{Th}$  normalized fluxes (Figure 10). As predicted for this situation, the  $^{230}\text{Th}$  normalized fluxes of lithogenic material obtained on Bermuda Rise ( $16 \text{ g m}^{-2} \text{ year}^{-1}$ ) are much higher than the flux of lithogenic material originating from surface waters. The latter can be estimated from the flux of lithogenic material ( $2 \text{ g m}^{-2} \text{ year}^{-1}$ ) measured with a sediment trap deployed at 3200 m (1300 m above the seafloor) at station OFP ( $32^\circ 05' \text{N}$ ,  $64^\circ 15' \text{W}$ ; *Conte et al.* [2001]), and from the  $^{230}\text{Th}$  normalized flux of lithogenic material obtained from the Holocene section of a core from the same general area (CHN82 31 11PC;  $42^\circ 23' \text{N}$ ,  $31^\circ 48' \text{W}$ ) but outside the drift deposit ( $1.9 \text{ g m}^{-2} \text{ year}^{-1}$ ; *Francois and Bacon* [1994]). The  $^{230}\text{Th}$  normalized carbonate fluxes, however, are comparable ( $\sim 7 \text{ g m}^{-2} \text{ year}^{-1}$ ) to the carbonate flux measured by sediment traps at station OFP ( $7.4 \text{ g m}^{-2} \text{ year}^{-1}$ ; *Conte et al.* [2001]). It is interesting to note that even though the sedimentation rates (and thus the focusing factors) are different in the two cores, they both give the same  $^{230}\text{Th}$  normalized fluxes. This must indicate

that the difference in focusing between the two cores is due to a local redistribution effect and not different input from distal nepheloid transport. The latter establishes the  $^{230}\text{Th}$  concentration of the sediment reaching the Rise. However, further redistribution after initial deposition on the Rise can produce variable sediment accumulation rates on the Rise, without changing the  $^{230}\text{Th}$  normalized rain rates. Thomson *et al.* [1999] also found similar  $^{230}\text{Th}$  normalized fluxes in two cores taken on the slope off Portugal at different depths (2465 m; 3381 m) and subjected to different degree of sediment focusing. This important study demonstrates the applicability of  $^{230}\text{Th}$  normalization to reconstruct vertical particle fluxes at ocean margins.

[64] The  $^{230}\text{Th}$  normalization model also assumes that the redistributed sediment has not been subjected to fractionation according to size, density or composition. Some degree of particle sorting is no doubt occurring, however, during sediment redistribution by bottom currents. Smaller grain sizes with larger surface areas and higher  $^{230}\text{Th}$  activities are preferentially redistributed [Thomson *et al.*, 1993; Scholten *et al.*, 1994; Luo and Ku, 1999]. Consequently,  $^{230}\text{Th}$  normalized fluxes could deviate from  $P^{\text{FV}}$ , even during redistribution in bottom nepheloid layers. Fortunately, fine-grained material generally constitutes the bulk of most deep-sea sediments, and it is unlikely that the hydrodynamically mobile fraction has a mean chemical and particle size composition very different from the bulk sediment from which it originates. This would be particularly true if syndepositional redistribution affects primarily phytodetritus aggregates, which would limit sorting of individual particles. To the extent that this is true,  $^{230}\text{Th}$  normalized fluxes would still be an accurate estimate of  $P^{\text{FV}}$ . However, the effect of sorting cannot be neglected for the occasional larger particles, such as large foraminifera or ice-rafted debris, which could reach the seafloor as discrete particles. These large particles are much less prone to lateral redistribution [Thomson *et al.*, 1993]. Since they are associated with only a small fraction of the total adsorbed  $^{230}\text{Th}$ , normalization to  $^{230}\text{Th}$  cannot be used to estimate their  $P^{\text{FV}}$  and focusing factor. A correction of the rain rates of such large particles by focusing factors based on the budget of  $^{230}\text{Th}$  adsorbed to small particles would overcompensate for their limited lateral transport.

## 5. Summary and Conclusion

[65] The rapidly increasing database on  $^{230}\text{Th}$  concentration in dated deep-sea sediment cores indicates that syndepositional redistribution of sediment by bottom currents is much more common than generally believed and must be systematically evaluated when the flux of sedimentary constituents is interpreted in terms of particle flux from the overlying surface water. Normalization to  $^{230}\text{Th}$  was proposed nearly twenty years ago as a means of assessing sediment redistribution and estimating the vertical rain rate of sedimentary constituents [Bacon, 1984]. The underlying principle of the method (i.e., the settling flux of scavenged  $^{230}\text{Th}$  is constant and equivalent to its rate of production) has now been verified to hold true within 30% over large areas of the ocean. This conclusion was reached by a variety of approaches ( $^{230}\text{Th}$  measurements in the water column

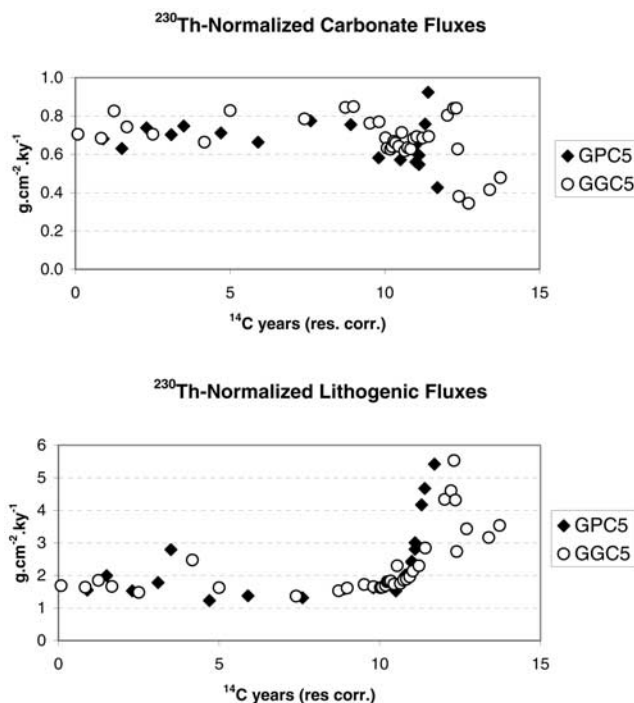


**Figure 10.** Comparison of  $^{230}\text{Th}$  normalized fluxes obtained from two cores taken in close proximity on Bermuda Rise (KNR 31 GPC5; 33°41'N, 57°37'W, 4583 m and OC326 GGC 5; 33°42'N, 57°35'W, 4550 m). The two cores have very different sedimentation rates (GPC 5: 19 cm kyr<sup>-1</sup>; GGC 5: 9 cm kyr<sup>-1</sup>) but similar  $^{230}\text{Th}$ -normalized fluxes.

and material intercepted by sediment traps; general circulation models), and is also supported by theoretical arguments. This level of uncertainty is adequate to identify sediment focusing, which often alters sediment mass accumulation rates several-fold. Errors resulting from assuming a flux equivalent to the known production rate of  $^{230}\text{Th}$  are systematic, not random, and will be further reduced as we improve our understanding of the limited lateral transport of  $^{230}\text{Th}$  in the water column. The general applicability of this method has now been convincingly established for much of the seafloor. Problems may arise, however, when it is applied to shallow sediments with high lithogenic content, and older sediments with high authigenic U content, because of difficulties in accurately measuring  $A_{\text{Th-230}}^{\text{scav}}$  in these sediments.  $^{230}\text{Th}$  normalization should not be applied to the coarse fraction of sediments that are minimally redistributed by bottom currents and scavenge very little  $^{230}\text{Th}$  because of their small surface area. In sediments heavily affected by focusing, such as drift deposits, the interpretation of the  $^{230}\text{Th}$  normalized flux should also consider the depth of lateral transport. If lateral transport occurs near the seafloor in bottom nepheloid layers,  $^{230}\text{Th}$  normalized fluxes approach the true vertical flux originating from the surface mixed layer. If lateral transport occurs at shallow depth in intermediate nepheloid layers,  $^{230}\text{Th}$  normalized fluxes approach the total flux (i.e., the vertical flux + lateral contributions). In addition to compensating for

sediment redistribution, <sup>230</sup>Th normalization has also the advantages of not relying on measurements of dry bulk density, of being less sensitive to chronological errors, and of providing higher resolution flux profiles. These advantages and recent analytical developments that greatly facilitate the measurement of <sup>230</sup>Th in sediments should prove to be powerful incentives for the widespread use of this

method in paleoceanographic studies and for the interpretation of sedimentary fluxes during the late Quaternary.

[66] **Acknowledgments.** R. Francois and M. P. Bacon acknowledge support from the National Science Foundation. M. Frank thanks the Swiss Science Foundation for support. The paper benefited from constructive reviews by R. F. Anderson and G. M. Henderson. This is WHOI contribution 11053.

## References

- Anderson, R. F. (1982), Concentration, vertical flux, and remineralization of particulate uranium in seawater, *Geochim. Cosmochim. Acta*, **46**, 1293–1299.
- Anderson, R. F., M. P. Bacon, and P. G. Brewer (1983), Removal of Th-230 and Pa-231 from the open ocean, *Earth Planet. Sci. Lett.*, **62**, 7–23.
- Anderson, R. F., Y. Lao, W. S. Broecker, S. Trumbore, H. J. Hofmann, and W. Wolfli (1990), Boundary scavenging in the Pacific Ocean: A comparison of Be-10 and Pa-231, *Earth Planet. Sci. Lett.*, **96**, 287–304.
- Anderson, R. F., N. Kumar, R. A. Mortlock, P. N. Froelich, P. W. Kubik, and M. Suter (1998), Late Quaternary changes in productivity of the Southern Ocean, *J. Mar. Sys.*, **17**, 497–514.
- Asmus, T., M. Frank, C. Koschmieder, N. Frank, R. Gersonde, G. Kuhn, and A. Mangini (1999), Variations of biogenic particle flux in the southern Atlantic section of the Subantarctic Zone during the late Quaternary: Evidence from sedimentary <sup>231</sup>Pa<sub>ex</sub> and <sup>230</sup>Th<sub>ex</sub>, *Mar. Geol.*, **159**, 63–78.
- Bacon, M. P. (1984), Glacial to interglacial changes in carbonate and clay sedimentation in the Atlantic Ocean estimated from <sup>230</sup>Th measurements, *Isotope Geosci.*, **2**, 97–111.
- Bacon, M. P. (1988), Tracers of chemical scavenging in the ocean: Boundary effects and large-scale chemical fractionation, *Philos. Trans. R. Soc. London A*, **325**, 147–160.
- Bacon, M. P., and R. F. Anderson (1982), Distribution of thorium isotopes between dissolved and particulate forms in the deep sea, *J. Geophys. Res.*, **87**, 2045–2056.
- Bacon, M. P., and J. N. Rosholt (1982), Accumulation rates of Th-230, Pa-231 and some transition metals on the Bermuda Rise, *Geochim. Cosmochim. Acta*, **46**, 651–666.
- Bacon, M. P., C.-H. Huh, A. P. Fleer, and W. G. Deuser (1985), Seasonality in the flux of natural radionuclides and plutonium in the deep Sargasso Sea, *Deep Sea Res.*, **32**, 273–286.
- Bareille, G., M. Labracherie, P. Bertrand, L. Labeyrie, G. Lavaux, and M. Dignan (1998), Glacial-interglacial changes in the accumulation rates of major biogenic components in Southern Indian Ocean sediments, *J. Mar. Sys.*, **17**, 527–539.
- Barnes, C. E., and J. K. Cochran (1990), Uranium removal in oceanic sediments and the oceanic U balance, *Earth Planet. Sci. Lett.*, **97**, 94–101.
- Beaulieu, S. E. (2002), Accumulation and fate of phytodetritus on the seafloor, *Oceanogr. Mar. Biol. Annu. Rev.*, **40**, 171–232.
- Biscaye, P. E., and S. Eitrem (1977), Suspended particulate loads and transport in the nepheloid layer of the abyssal Atlantic Ocean, *Mar. Geol.*, **23**, 155–172.
- Chabaux, F., J. Riotte, and O. Dequincey (2003), U-Th-Ra fractionations during weathering and river, *Rev. Mineral. Geochem.*, **52**, 533–576.
- Chase, Z., R. F. Anderson, and M. Q. Fleisher (2001), Evidence from authigenic uranium for increased productivity of the glacial Subantarctic Ocean, *Paleoceanography*, **16**, 468–478.
- Chase, Z., R. F. Anderson, M. Q. Fleisher, and P. W. Kubik (2003), Scavenging of <sup>230</sup>Th, <sup>231</sup>Pa and <sup>10</sup>Be in the southern ocean (SW Pacific sector): The importance of particle flux, particle composition and advection, *Deep Sea Res. Part II*, **50**, 739–768.
- Cheng, H., R. L. Edwards, J. Hoff, C. D. Gallup, D. A. Richards, and Y. Asmerom (2000), The half lives of uranium-234 and thorium-230, *Chem. Geol.*, **169**, 17–33.
- Choi, M.-S., R. Francois, K. Sims, M. P. Bacon, S. Brown-Leger, A. P. Fleer, L. Ball, D. Schneider, and S. Pichat (2001), Rapid determination of <sup>230</sup>Th and <sup>231</sup>Pa in seawater by desolvated-micronebulization Inductively-Coupled Magnetic Sector Mass Spectrometry, *Mar. Chem.*, **76**, 99–112.
- Cochran, J. K., and S. Krishnaswami (1980), Radium, thorium, uranium and Pb-210 in deep-sea sediments and sediment pore waters from the North Equatorial Pacific, *Am. J. Sci.*, **280**, 849–889.
- Conte, M., N. Ralph, and E. H. Ross (2001), Seasonal and interannual variability in deep ocean particle fluxes at the Oceanic Flux Program (OFP)/Bermuda Atlantic Time Series (BATS) site in the western Sargasso Sea near Bermuda, *Deep Sea Res. Part II*, **48**, 1471–1505.
- Curry, W. B., and G. P. Lohmann (1986), Late Quaternary carbonate sedimentation at the Sierra Leone Rise (eastern equatorial Atlantic Ocean), *Mar. Geol.*, **70**, 223–250.
- DeMaster, D. J. (1981), The supply and accumulation of silica in the marine environment, *Geochim. Cosmochim. Acta*, **45**, 1715–1732.
- DeMaster, D. J. (2002), The accumulation and cycling of biogenic silica in the Southern Ocean: Revisiting the marine silica budget, *Deep Sea Res. Part II*, **49**, 3155–3168.
- Dezileau, L., G. Bareille, J.-L. Reyss, and F. Lemoine (2000), Evidence for strong sediment redistribution by bottom currents along the southeast Indian ridge, *Deep Sea Res. Part I*, **47**, 1899–1936.
- Dickson, R. R., and I. N. McCave (1986), Nepheloid layers on the continental slope west of Porcupine Bank, *Deep Sea Res.*, **33**, 791–818.
- Diekmann, B., G. Kuhn, A. Mackensen, R. Petschik, D. K. Fütterer, R. Gersonde, C. Rühlemann, and H. S. Niebler (1999), Kaolin and chlorite as tracers of modern and late Quaternary deep water circulation in the South Atlantic and the adjoining Southern Ocean, in *Use of Proxies in Paleoceanography: Examples From the South Atlantic*, edited by G. Fisher and G. Wefer, pp. 285–313, Springer-Verlag, New York.
- Doney, S. C., and W. J. Jenkins (1994), Ventilation of the Deep Western Boundary Current and abyssal western North Atlantic: Estimates from Tritium and <sup>3</sup>He distributions, *J. Phys. Oceanogr.*, **24**, 638–659.
- Dunk, R. M., R. A. Mills, and W. J. Jenkins (2002), A reevaluation of the oceanic uranium budget for the Holocene, *Chem. Geol.*, **190**, 45–67.
- Ewing, J., and M. Ewing (1970), Seismic reflection, in *The Sea*, vol. 4, part I, edited by A. E. Maxwell, pp. 1–51, John Wiley, Hoboken, N. J.
- Ewing, M., J. Ewing, and M. Talwani (1964), Sediment distribution in the oceans: The Mid-Atlantic Ridge, *Bull. Geol. Soc. Am.*, **75**, 17–35.
- Francois, R., and M. P. Bacon (1991), Variations in terrigenous input to the deep equatorial Atlantic during the past 24,000 years, *Science*, **251**, 1473–1476.
- Francois, R., and M. P. Bacon (1994), Heinrich events in the North Atlantic: Radiochemical evidence, *Deep Sea Res. Part I*, **41**, 315–334.
- Francois, R., M. P. Bacon, and D. O. Suman (1990), Th-230 profiling in deep-sea sediments: High-resolution records of flux and dissolution of carbonate in the equatorial Atlantic during the last 24,000 years, *Paleoceanography*, **5**, 761–787.
- Francois, R., M. P. Bacon, M. A. Altabet, and L. D. Labeyrie (1993), Glacial/interglacial changes in sediment rain rate in the SW Indian sector of subantarctic waters as recorded by <sup>230</sup>Th, <sup>231</sup>Pa, U and δ<sup>15</sup>N, *Paleoceanography*, **8**, 611–629.
- Francois, R., M. A. Altabet, E.-F. Yu, D. Sigman, M. P. Bacon, M. Frank, G. Bohrmann, G. Bareille, and L. D. Labeyrie (1997), Contribution of southern ocean surface water stratification to low atmospheric CO<sub>2</sub> concentrations during the last glacial period, *Nature*, **389**, 929–935.
- Frank, M., A. Eisenhauer, W. J. Bonn, P. Walter, H. Grobe, P. W. Kubik, B. Ditttrich-Hannen, and A. Mangini (1995), Sediment redistribution versus paleoproductivity change: Weddell Sea margin sediment stratigraphy and biogenic particle flux of the last 25,000 years deduced from <sup>230</sup>Th<sub>ex</sub>, <sup>10</sup>Be and biogenic barium profiles, *Earth Planet. Sci. Lett.*, **136**, 559–573.
- Frank, M., R. Gersonde, M. Rutgers van der Loeff, G. Kuhn, and A. Mangini (1996), Late Quaternary sediment dating and quantification of lateral sediment redistribution applying <sup>230</sup>Th<sub>ex</sub>: A study from the eastern Atlantic sector of the Southern Ocean, *Geol. Rundsch.*, **85**, 554–566.
- Frank, M., R. Gersonde, and A. Mangini (1999), Sediment redistribution, <sup>230</sup>Th-normalization and implication for the reconstruction of particle flux and export productivity, in *Use of Proxies in Paleoceanography: Examples From the South Atlantic*, edited by G. Fisher and G. Wefer, pp. 409–426, Springer-Verlag, New York.

- Frank, M., R. Gersonde, M. Rutgers van der Loeff, G. Bohrmann, C. Nürnberg, P. W. Kubik, M. Suter, and A. Mangini (2000), Similar glacial and interglacial export bioproductivity in the Atlantic sector of the Southern Ocean: Multiproxy evidence and implications for atmospheric CO<sub>2</sub>, *Paleoceanography*, *15*, 642–658.
- Froelich, P. N., et al. (1991), Biogenic opal and carbonate accumulation rates in the subantarctic south Atlantic: The late Neogene of Meteor Rise Site 704, *Proc. Ocean Drill. Program Sci. Results*, *114*, 515–550.
- Gersonde, R., et al. (2003), Last glacial sea surface temperatures and sea-ice extent in the Southern Ocean (Atlantic-Indian sector): A multiproxy approach, *Paleoceanography*, *18*(3), 1061, doi:10.1029/2002PA000809.
- Hays, J. D., J. Imbrie, and N. J. Shackleton (1976), Variations in the Earth's orbit: Pacemakers of the ice ages, *Science*, *194*, 1121–1132.
- Henderson, G. M., and R. F. Anderson (2003), The U-series toolbox for paleoceanography, *Rev. Mineral. Geochem.*, *52*, 493–531.
- Henderson, G. M., C. Heinze, R. F. Anderson, and A. M. E. Winguth (1999), Global distribution of the <sup>230</sup>Th flux to ocean sediments constrained by GCM modeling, *Deep Sea Res. Part I*, *46*, 1861–1893.
- Hinrichs, J., and B. Schnetger (1999), A fast method for the simultaneous determination of <sup>230</sup>Th, <sup>234</sup>U, and <sup>235</sup>U with isotope dilution sector field ICP-MS, *Analyst*, *124*, 927–932.
- Honjo, S., J. Dymond, R. Collier, and S. J. Manganini (1995), Export production of particles to the interior of the equatorial Pacific Ocean during the 1992 EqPac experiment, *Deep Sea Res. Part II*, *42*, 831–870.
- Hyun, S., S.-J. Han, and A. Taira (2002), Barium in hemipelagic sediment of the northwest Pacific: Coupling with biogenic carbonate, *Paleoceanography*, *17*(4), 1066, doi:10.1029/2001PA000651.
- Ikehara, M., K. Kawamura, N. Ohkouchi, M. Murayama, T. Nakamura, and A. Taira (2000), Variations of terrestrial input and marine productivity in the Southern Ocean (48°S) during the last two deglaciations, *Paleoceanography*, *15*, 170–180.
- Klinkhammer, G., and M. R. Palmer (1991), Uranium in the Oceans: Where it goes and why, *Geochim. Cosmochim. Acta*, *55*, 1799–1806.
- Krishnaswami, S. (1976), Authigenic transition elements in Pacific pelagic clays, *Geochim. Cosmochim. Acta*, *40*, 425–434.
- Krishnaswami, S., D. Lal, B. L. K. Somayajulu, R. Weiss, and H. Craig (1976), Large-volume in-situ filtration of deep Pacific waters: Mineralogical and radioisotope studies, *Earth Planet. Sci. Lett.*, *32*, 420–429.
- Kumar, N., R. Gwiazda, R. F. Anderson, and P. N. Froelich (1993), <sup>231</sup>Pa/<sup>230</sup>Th ratios in sediments as a proxy for past changes in southern ocean productivity, *Nature*, *362*, 45–48.
- Kumar, N., R. F. Anderson, R. A. Mortlock, P. N. Froelich, P. W. Kubik, B. Dittrich-Hannen, and M. Suter (1995), Iron fertilization of glacial-age Southern Ocean productivity, *Nature*, *378*, 675–680.
- Latimer, J. C., and G. M. Filipelli (2001), Terrigenous input and paleoproductivity in the Southern Ocean, *Paleoceanography*, *16*, 625–641.
- Luo, S., and T.-L. Ku (1999), Oceanic <sup>231</sup>Pa/<sup>230</sup>Th ratio influenced by particle composition and remineralization, *Earth Planet. Sci. Lett.*, *167*, 183–195.
- Lyle, M. W., and J. Dymond (1976), Metal accumulation rates in the southeast Pacific—errors introduced from assumed bulk densities, *Earth Planet. Sci. Lett.*, *30*, 164–168.
- Lyle, M., D. W. Murray, B. P. Finney, J. Dymond, J. M. Robbins, and K. Brooksforce (1988), The record of late Pleistocene biogenic sedimentation in the eastern tropical Pacific Ocean, *Paleoceanography*, *3*, 39–59.
- Lyle, M., A. Mix, and N. Piasias (2002), Patterns of CaCO<sub>3</sub> deposition in the eastern tropical Pacific Ocean for the last 150 kyr: Evidence for a southeast Pacific depositional spike during marine isotope stage (MIS) 2, *Paleoceanography*, *17*(2), 1013, doi:10.1029/2000PA000538.
- Mangini, A., and L. Diester-Haass (1983), Excess Th-230 in sediments off NW Africa traces upwelling in the past, in *Coastal Upwelling: Its Sediment Record. Part A: Responses of the Sedimentary Regime to Present Coastal Upwelling*, edited by E. Suess and J. Thiede, pp. 455–466, Plenum, New York.
- Marcantonio, F., N. Kumar, M. Stute, R. F. Anderson, M. A. Seidl, P. Schlosser, and A. C. Mix (1995), A comparative study of accumulation rates derived by He and Th isotope analysis of marine sediments, *Earth Planet. Sci. Lett.*, *133*, 549–555.
- Marcantonio, F., R. R. Anderson, M. Stute, N. Kumar, P. Schlosser, and A. C. Mix (1996), Extraterrestrial <sup>3</sup>He as a tracer of marine sediment transport and accumulation, *Nature*, *383*, 705–707.
- Marcantonio, F., R. F. Anderson, S. Higgins, M. Stute, P. Schlosser, and P. W. Kubik (2001a), Sediment focusing in the central equatorial Pacific ocean, *Paleoceanography*, *16*, 260–267.
- Marcantonio, F., R. F. Anderson, S. Higgins, M. Q. Fleisher, M. Stute, and P. Schlosser (2001b), Abrupt intensification of the SW Indian Ocean monsoon during the last deglaciation: Constraints from Th, Pa, and He isotopes, *Earth Planet. Sci. Lett.*, *184*, 505–514.
- Marchal, O., R. Francois, T. F. Stocker, and F. Joos (2000), Ocean thermohaline circulation and sedimentary <sup>231</sup>Pa/<sup>230</sup>Th ratio, *Paleoceanography*, *15*, 625–641.
- McCave, I. N. (1986), Local and global aspects of the bottom nepheloid layers in the world ocean, *Neth. J. Sea Res.*, *20*, 167–181.
- McManus, J., R. F. Anderson, W. S. Broecker, M. Q. Fleisher, and S. Higgins (1998), Radio-metrically determined sedimentary fluxes in the sub-polar North Atlantic during the last 140,000 years, *Earth Planet. Sci. Lett.*, *155*, 29–43.
- Mollenhauer, G., R. R. Schneider, P. J. Muller, V. Spiess, and G. Wefer (2002), Glacial/interglacial variability in the Benguela upwelling system: Spatial distribution and budgets of organic carbon accumulation, *Global Biogeochem. Cycles*, *16*(4), 1134, doi:10.1029/2001GB001488.
- Moran, S. B., M. A. Charette, J. A. Hoff, R. L. Edwards, and W. M. Landing (1997), Distribution of <sup>230</sup>Th in the Labrador Sea and its relation to ventilation processes: Constraints on <sup>231</sup>Pa/<sup>230</sup>Th as a paleocirculation tracer in the deep Atlantic, *Earth Planet. Sci. Lett.*, *150*, 151–160.
- Moran, S. B., C.-C. Shen, H. N. Edmonds, S. E. Weinstein, J. N. Smith, and R. L. Edwards (2002), Dissolved and particulate <sup>231</sup>Pa and <sup>230</sup>Th in the Atlantic Ocean: Constraints on intermediate/deep water age, boundary scavenging, and <sup>231</sup>Pa/<sup>230</sup>Th fractionation, *Earth Planet. Sci. Lett.*, *203*, 999–1014.
- Mortlock, R. A., C. D. Charles, P. N. Froelich, M. A. Zibello, J. Saltzman, J. D. Hays, and L. H. Burckle (1991), Evidence for lower productivity in the Antarctic Ocean during the last Glaciation, *Nature*, *351*, 220–223.
- Nozaki, Y., and T. Nakanishi (1985), <sup>231</sup>Pa and <sup>230</sup>Th profiles in the open ocean water column, *Deep Sea Res.*, *32*, 1209–1220.
- Nozaki, Y., Y. Horibe, and H. Tsubota (1981), The water column distributions of thorium isotopes in the western North Pacific, *Earth Planet. Sci. Lett.*, *54*, 203–216.
- Pak, H., J. R. Zanefeld, and J. Kitchen (1980), Intermediate nepheloid layers observed off Oregon and Washington, *J. Geophys. Res.*, *85*, 6697–6708.
- Paytan, A., M. Kastner, and F. P. Chavez (1996), Glacial to interglacial fluctuations in productivity in the equatorial Pacific as indicated by marine barite, *Science*, *274*, 1355–1357.
- Petschick, R., G. Kuhn, and F. Gingele (1996), Clay mineral distribution in surface sediments of the South Atlantic: Sources, transport, and relation to oceanography, *Mar. Geol.*, *130*, 203–229.
- Pondaven, P., O. Ragueneau, P. Treguer, A. Hauvespre, L. Dezileau, and J.-L. Reyss (2000), Resolving the “opal paradox” in the Southern Ocean, *Nature*, *405*, 168–172.
- Rea, D. K., and M. Leinen (1988), Asian aridity and the zonal westerlies: Late Pleistocene and Holocene record of eolian deposition in the northwest Pacific Ocean, *Palaeoogeogr. Palaecoclimatol. Palaeoecol.*, *66*, 1–8.
- Robinson, L. F., N. S. Belshaw, and G. M. Henderson (2004), U and Th concentrations and isotope ratios in modern carbonates and waters from the Bahamas, *Geochimica Cosmochimica Acta*, in press.
- Rosenthal, Y., E. A. Boyle, L. Labeyrie, and D. Oppo (1995), Glacial enrichments of authigenic Cd and U in Subantarctic sediments: A climatic control on the elements' oceanic budget?, *Paleoceanography*, *10*, 395–413.
- Roy-Barman, M. J. H., J. H. Chen, and G. J. Wasserburg (1996), <sup>230</sup>Th-<sup>232</sup>Th systematics in the central Pacific Ocean: The sources and the fates of thorium, *Earth Planet. Sci. Lett.*, *139*, 351–363.
- Rühlemann, C., M. Frank, W. Hale, A. Mangini, S. Mulitza, P. J. Müller, and G. Wefer (1996), Late Quaternary productivity changes in the western equatorial Atlantic: Evidence from <sup>230</sup>Th normalized carbonate and organic carbon accumulation rates, *Mar. Geol.*, *135*, 127–152.
- Rutgers van der Loeff, M. M., and G. W. Berger (1993), Scavenging of <sup>230</sup>Th and <sup>231</sup>Pa near the Antarctic Polar Front in the South Atlantic, *Deep Sea Res. Part II*, *40*, 339–357.
- Sarmiento, J. L., C. G. H. Rooth, and W. S. Broecker (1982), Radium-228 as a tracer of basin wide processes in the abyssal ocean, *J. Geophys. Res.*, *87*, 9694–9698.
- Sarnthein, M., K. Winn, J.-C. Duplessy, and M. R. Fontugne (1988), Global variations of surface ocean productivity in low and mid latitudes: Influence on CO<sub>2</sub> reservoirs of the deep ocean and atmosphere during the last 21,000 years, *Paleoceanography*, *3*, 361–399.
- Scholten, J. C., H. Bohrmann, R. Botz, A. Mangini, H. Paetsch, P. Stoffers, and E. Vogelsang (1990), High resolution Th-230 stratigraphy of sediments from high latitude areas (Norwegian Sea, Fram Strait), *Earth Planet. Sci. Lett.*, *101*, 54–62.

- Scholten, J. C., R. Botz, H. Paetsch, and P. Stoffers (1994),  $^{230}\text{Th}_{\text{ex}}$  flux into Norwegian-Greenland Sea sediments: Evidence for lateral sediment transport during the past 300,000 years, *Mar. Geol.*, *121*, 111–124.
- Scholten, J. C., A. Michel, and M. Rutgers van der Loeff (1995), Distribution of  $^{230}\text{Th}$  and  $^{231}\text{Pa}$  in the water column in relation to the ventilation of the deep Arctic basins, *Deep Sea Res. Part II*, *42*, 1519–1531.
- Scholten, J. C., J. Fietzke, S. Vogler, M. M. Rutgers van der Loeff, A. Mangini, W. Koeve, J. Waniek, P. Stoffers, A. Antia, and J. Kuss (2001), Trapping efficiencies of sediment traps from the deep eastern North Atlantic: The  $^{230}\text{Th}$  calibration, *Deep Sea Res. Part II*, *48*, 2383–2408.
- Shaw, T. J., and R. Francois (1991), A fast and sensitive ICP-MS assay for the determination of  $^{230}\text{Th}$  in marine sediments, *Geochim. Cosmochim. Acta*, *55*, 2075–2078.
- Shen, C.-C., R. L. Edwards, H. Cheng, J. A. Dorale, R. B. Thomas, S. B. Moran, S. E. Weinstein, and H. N. Edmonds (2002), Uranium and thorium isotopic and concentration measurements by magnetic sector inductively coupled plasma mass spectrometry, *Chem. Geol.*, *185*, 165–178.
- Spencer, D. W., M. P. Bacon, and P. G. Brewer (1981), Models of distribution of  $^{210}\text{Pb}$  in a section across the North Equatorial Atlantic Ocean, *J. Mar. Res.*, *38*, 119–138.
- Suman, D. O., and M. P. Bacon (1989), Variations in Holocene sedimentation in the North American basin determined from  $^{230}\text{Th}$  measurements, *Deep Sea Res.*, *36*, 869–878.
- Thomas, E., K. K. Turekian, and K.-Y. Wei (2000), Productivity control of fine particle transport to equatorial Pacific sediment, *Global Biogeochem. Cycles*, *14*, 945–955.
- Thomson, J., S. Colley, R. Anderson, G. T. Cook, A. B. Mackenzie, and D. D. Harkness (1993), Holocene sediment fluxes in the NE Atlantic from  $^{230}\text{Th}_{\text{excess}}$  and radiocarbon measurements, *Paleoceanography*, *8*, 631–650.
- Thomson, J., S. Colley, R. Anderson, and G. T. Cook (1995), A comparison of sediment accumulation chronologies by the radiocarbon and  $^{230}\text{Th}_{\text{ex}}$  methods, *Earth Planet. Sci. Lett.*, *133*, 59–70.
- Thomson, J., S. Nixon, C. P. Summerhayes, J. Schonfeld, R. Zahn, and P. M. Grootes (1999), Implications for sedimentation changes on the Iberian margin over the last two glacial/interglacial transitions from ( $^{230}\text{Th}_{\text{excess}}$ )<sub>0</sub> systematics, *Earth Planet. Sci. Lett.*, *165*, 255–270.
- Vogler, S., J. C. Scholten, and A. Mangini (1998),  $^{230}\text{Th}$  in the eastern North Atlantic: The importance of water mass ventilation in the balance of  $^{230}\text{Th}$ , *Earth Planet. Sci. Lett.*, *156*, 61–74.
- Walsh, I., K. Fischer, D. Murray, and J. Dymond (1988), Evidence for resuspension of rebound particles from near-bottom sediment traps, *Deep Sea Res.*, *35*, 59–70.
- Walter, H. J., W. Geibert, M. M. Rutgers van der Loeff, G. Fischer, and U. Bathmann (2001), Shallow versus deep water scavenging of  $^{231}\text{Pa}$  and  $^{230}\text{Th}$  in radionuclide enriched waters of the Atlantic sector of the Southern Ocean, *Deep Sea Res. Part I*, *48*, 471–493.
- Yu, E.-F., R. Francois, M. P. Bacon, and A. P. Fleer (2001), Fluxes of  $^{230}\text{Th}$  and  $^{231}\text{Pa}$  to the deep sea: Implications for the interpretation of excess  $^{230}\text{Th}$  and  $^{231}\text{Pa}/^{230}\text{Th}$  profiles in sediments, *Earth Planet. Sci. Lett.*, *91*, 29–230.

---

M. P. Bacon and R. Francois, Department of Marine Chemistry and Geochemistry, Woods Hole Oceanographic Institution, Woods Hole, MA 02543, USA. (rfrancois@cliff.who.edu)

M. Frank, Department of Earth Sciences, ETH Zürich Institute for Isotope Geology and Mineral Resources, ETH-Zentrum, NO F51.3, CH-8092 Zürich, Switzerland.

M. M. Rutgers van der Loeff, Rijksinstituut voor Kust en Zee Kortenaerkade 1, Postbus 20907, N-2500 EX Den Haag, Netherlands.